Transition to turbulence in thermoconvection & aerodynamics

by *Emmanuel Plaut* at Mines Nancy

Version with elements of solutions of November 15, 2022

Contents

Introduction

This is the latest version of the lecture notes of Emmanuel Plaut for the module ***Transition to turbulence in thermoconvection and aerodynamics*** at **Mines Nancy**, in the Department Energy, at the Master 2 Level.

This module is somehow a follow up of the module ***Mécanique des fluides 2 : ondes, couches limites et turbulence*** (Plaut 2020) of the Master 1 Level. Indeed, one can find, in the chapter 3 of Plaut (2020), an introduction to instabilities. To fix some notions and our notations, a short chapter 0 is given at the beginning of these lecture notes.

We study the problem of the ***transition to spatio-temporal complexity*** and ***turbulence*** in fluid systems, either closed in chapter 1, or open in chapter 2. Somehow, we want to fill the gap between the 'academic' calculations of laminar flows and the 'engineering-oriented' calculations or computations of turbulent flows.
Chapter 1, which focusses on ***thermoconvection***, is also an occasion to increase our knowledge about ***heat transfers in fluids***. One question we want to answer is: if I heat a fluid layer from below, when and how thermoconvection flows set in ? This question matters, since we know that passing from conduction to convection increases heat transfers.
Chapter 2, which focusses on ***open shear flows***, is also an occasion to increase our knowledge in ***aerodynamics***. A relevant question in this domain is: if the Reynolds number that characterizes the flow around an airplane wing (an 'airfoil') or around a wind turbine blade increases, when and how the boundary layers attached to the wing or blade become turbulent ? This question matters, since we know that this transition implies a dramatic increase of the drag force, and changes the lift force.
We introduce, on these examples, the ***bifurcation theory***, or ***'catastrophe theory'***, which is of interest for all nonlinear dynamical systems in general... 'Standard' dynamical systems governed by ordinary differential equations, or 'extended' dynamical systems governed by partial differential equations. Of course, 'fluid systems' are 'extended dynamical systems'...
In order to obtain approximate solutions of the partial differential equations, the bifurcation theory relies on a ***'weakly nonlinear approach'***. It starts with a ***linear stability analysis*** and treats the nonlinear terms as small perturbations. Since we focus on highly symmetric systems, typically, systems that are invariant by translations (in the x-direction), we can use ***'normal modes'*** at the linear stage. Because we also consider only problems with 2 spatial dimensions (x and z), we end up with ordinary differential equations. In some rare cases, like Rayleigh-Bénard thermoconvection with slip boundary conditions, these equations can be solved analytically. Then, the weakly nonlinear analysis may be performed analytically: this is an occasion to perform a few ***formal*** (symbolic) ***computations*** with **Mathematica**. Most often, the equations of the linear

analysis demand a numerical solution... this is the case for open shear flows ! We consider this as an opportunity to introduce a (new for the students) ***numerical method***, the ***'spectral method'***, which we also program with **Mathematica**. This is an occasion to increase our skills in numerics. Similar approaches are used in the ***'spectral element methods'***, which are competitive methods for computational fluid dynamics[1].
To conclude, I mention that I gave in the past a module with a similar content in french. It may be interesting, for some students, to refer to the corresponding lecture notes Plaut (2008).

The aim of this document is to give a framework for the lectures. Many exercises, and the problem 2.1 for instance, will be solved during the sessions. Their solution are displayed in the 'video presentations' posted on the ***dynamic web page of the module***[2]

http://emmanuelplaut.perso.univ-lorraine.fr/t2t

after the sessions. However, in this ***final version of the lecture notes, pieces of solutions of all exercises and problems are included***, e.g. in equation (1.34) and figure 1.2.

I thank Luca Brandt from KTH for providing a copy of Schlatter *et al.* (2010).

Nancy, November 16, 2022.
Emmanuel Plaut.

[1]For instance **nek5000** is a state-of-the-art open source code that can realize very accurate DNS: check https://nek5000.mcs.anl.gov .

[2]Please also check this page for new versions of these lecture notes, and for the planning of this module. Ignore in this final version of the notes the 'DIY' in the legend of some figures, which meant 'Do it yourself' and were some incitements to involve the students; in their paper copy of the lecture notes, the corresponding figures were empty...

Chapter 0

The basic concepts and equations of fluid dynamics - Notations

0.1 Cartesian coordinates, tensors and differential operators

We use a ***cartesian system of coordinates*** of origin O, associated to the laboratory frame. The coordinates are denoted (x, y, z) or (x_1, x_2, x_3), and we use Einstein's convention of summation over repeated indices, e.g. the position vector is

$$\mathbf{x} \;=\; x_i \mathbf{e}_i$$

with $\mathbf{e}_1$, $\mathbf{e}_2$, $\mathbf{e}_3$ or $\mathbf{e}_x$, $\mathbf{e}_y$, $\mathbf{e}_z$ the orthonormal base vectors. Vectors (e.g., $\mathbf{x}$) and tensors of order 2 (linear applications from $\mathbb{R}^3$ to $\mathbb{R}^3$, e.g., $\boldsymbol{\sigma}$, see the equation 0.2) are simply denoted by boldface characters. The use of tensorial intrinsic notations is minimized, to save some energy to face other difficulties.
Last but not least, ∂_t (resp. ∂_{x_i}) denotes the differential operator that takes the partial derivative with respect to the time t (resp. coordinate x_i).

0.2 Dynamics of incompressible newtonian fluids

The ***eulerian velocity field*** $\mathbf{v}(\mathbf{x}, t)$ is used to describe the flow of ***incompressible*** or ***weakly compressible newtonian fluids***. In this latter case, the ***mass density*** ρ depends weakly on the temperature, as it will be precised in the chapter 1. However, the ***incompressibility*** or ***weak compressibility*** means that the ***mass conservation equation*** always reads

$$\boxed{\partial_{x_i} v_i \;=\; 0} \;, \tag{0.1}$$

i.e., the velocity field $\mathbf{v}$ is 'conservative'.
The ***Cauchy stress tensor*** $\boldsymbol{\sigma}$ determines the surface force $d^2\mathbf{f}$ exerted on a small surface of area d^2A and normal unit vector $\mathbf{n}$ pointing outwards, by the exterior onto the interior, through

$$d^2\mathbf{f} \;=\; \boldsymbol{\sigma} \cdot \mathbf{n}\, d^2A \;=\; \sigma_{ij} n_j\; d^2A\; \mathbf{e}_i \;. \tag{0.2}$$

The stresses σ_{ij} are given by the sum of ***static pressure*** and ***viscous stresses***,

$$\sigma_{ij} \;=\; -\,p_{\text{static}} \delta_{ij} \;+\; \tau_{ij}(\mathbf{v}) \tag{0.3}$$

with τ_{ij} the components of the ***viscous stress tensor*** $\boldsymbol{\tau}$. It is given by

$$\boldsymbol{\tau}(\mathbf{v}) \;=\; 2\eta\mathbf{S}(\mathbf{v}) \tag{0.4}$$

with η the ***dynamic viscosity*** of the fluid, $\mathbf{S}(\mathbf{v})$ the ***rate-of-strain tensor*** defined as the symmetric part of the velocity gradient, i.e., in components,

$$\boxed{S_{ij}(\mathbf{v}) \;:=\; \frac{1}{2}(\partial_{x_i} v_j + \partial_{x_j} v_i)}\;. \tag{0.5}$$

In this equation, the sign := means a definition[1].
The ***linear momentum equation***[2] is the ***Navier-Stokes equation***

$$\boxed{\rho\frac{d\mathbf{v}}{dt} \;=\; \rho[\partial_t\mathbf{v} \;+\; (\mathbf{v}\cdot\boldsymbol{\nabla})\mathbf{v}] \;=\; \rho\mathbf{g} \;+\; \mathbf{div}\boldsymbol{\sigma}} \tag{0.6}$$

with $\mathbf{g}$ the ***acceleration due to gravity***. In components,

$$\rho[\partial_t v_i \;+\; v_j\partial_{x_j} v_i] \;=\; \rho g_i \;+\; \partial_{x_j}\sigma_{ij} \;=\; \rho g_i \;-\; \partial_{x_i} p_{\text{static}} \;+\; \partial_{x_j}(2\eta S_{ij}(\mathbf{v}))\;, \tag{0.7}$$

where g_i are the components of $\mathbf{g}$.
After dividing by the mass density, we get another form of the ***Navier-Stokes equation***,

$$\boxed{\partial_t v_i \;+\; v_j\partial_{x_j} v_i \;=\; g_i \;-\; \frac{1}{\rho}\partial_{x_i} p_{\text{static}} \;+\; \partial_{x_j}(2\nu S_{ij}(\mathbf{v}))} \tag{0.8}$$

with $\nu = \eta/\rho$ the ***kinematic viscosity*** of the fluid. The l.h.s.[3] is in fact the acceleration of the fluid particle (in the sense of the continuum mechanics) that passes through $\mathbf{x}$ at time t...
In chapter 1 we will consider ***weakly compressible fluids***, hence we will work with the static pressure field, denoted p instead of p_{static} to save space and energy.
On the contrary, in chapter 2 we will consider ***incompressible fluids***. A ***modified pressure*** that includes a gravity term,

$$p \;=\; p_{\text{static}} \;+\; \rho g Z\;, \tag{0.9}$$

where Z is a vertical coordinate, can then be used, to group the first two terms on the r.h.s. of equation (0.8), which reads therefore

$$\boxed{\partial_t v_i \;+\; v_j\partial_{x_j} v_i \;=\; -\,(1/\rho)\partial_{x_i} p \;+\; \nu\Delta v_i}\;, \tag{0.10}$$

or, intrinsically,

$$\boxed{\frac{d\mathbf{v}}{dt} \;=\; \partial_t\mathbf{v} \;+\; (\mathbf{v}\cdot\boldsymbol{\nabla})\mathbf{v} \;=\; -\,(1/\rho)\boldsymbol{\nabla} p \;+\; \nu\boldsymbol{\Delta}\mathbf{v}}\;. \tag{0.11}$$

[1] In french, $\mathbf{S}$ is the *tenseur des taux de déformation*, it was therefore denoted $\mathbf{D}$ in Plaut (2020).

[2] In french, the linear momentum is the *quantité de mouvement*, whereas the angular momentum is the *moment cinétique*.

[3] An equation reads generically l.h.s. = r.h.s. with l.h.s. its ‘left hand side’, r.h.s. its ‘right hand side’.

Chapter 1

Transition to spatio-temporal complexity in thermoconvection

This chapter corresponds to the sessions 1 *to* 3*.*

1.1 Generalities

1.1.1 Buoyancy force, geometry and physics

Thermoconvection or ***'natural convection'*** designates the flows that develop spontaneously in ***compressible fluids*** exposed to ***temperature gradients*** and ***gravity***. The 'motor' is thus the ***'buoyancy' force***, the first term in the r.h.s. of the ***Navier-Stokes equation*** (0.6)

$$\rho(T)\frac{d\mathbf{v}}{dt} \;=\; \rho(T)\;\mathbf{g} \;-\; \boldsymbol{\nabla} p \;+\; \mathbf{div}\boldsymbol{\tau} \tag{1.1}$$

with $\rho(T)$ the density, T the temperature, $\mathbf{v}$ the velocity, $\mathbf{g}$ the acceleration due to gravity, p the (static) pressure field and $\boldsymbol{\tau}$ the viscous stress tensor. During the oral lectures, a rapid analysis and presentation of ***thermoconvection phenomena*** will be given. In particular, we will show that static solutions, $\mathbf{v} = \mathbf{0}$, are possible only if

$$\boldsymbol{\nabla} T \times \mathbf{g} \;=\; \mathbf{0} \quad\Longleftrightarrow\quad \boldsymbol{\nabla} T \parallel \mathbf{g}\;. \tag{1.2}$$

If this is not the case, for instance, if $\boldsymbol{\nabla} T \perp \mathbf{g}$, thermoconvection flows always develop, even if the temperature gradients are quite small. This is the case in a ***differentially heated cavity***, where $\boldsymbol{\nabla} T$ is horizontal and $\mathbf{g}$ is vertical. Convection in a differentially heated cavity has been studied for instance by Davis (1983). It can be seen as a simplistic model of the problem of heating a room by a vertical radiator fixed to one of the sidewalls of this room.

The focus here is, instead, on ***Rayleigh-Bénard Thermoconvection*** (RBT; figure 1.1), where $\boldsymbol{\nabla} T$ and $\mathbf{g}$ are vertical. This is also a 'simple' closed fluid system, that permits well-controlled experiments. Because, according to (1.2), there exists a static, conduction state, thermoconvection can only come in through an ***instability*** of this state. This system has more degrees of freedom than the differentially heated cavity, where it is sure that, near the hot sidewall, there will be an upward flow. On the contrary, in a RBT cell, the position of the upward flow(s) may depend on very small 'initial' perturbations, or, even, change in a chaotic manner or due to 'secondary' instabilities. This renders this system quite interesting.

During the oral lectures, and, briefly, in section 1.7, we will mention phenomena in RBT cells in ***confined geometry***. Such cells have a very small lateral extension, for instance, a 'quasi 2D square' geometry with sidewalls at $x = \pm L_x = \pm d/2$, $y = \pm L_y \ll d$ with d the height of the cavity (figure 1.1).
In the core of this chapter, however, we consider RBT in an ***extended geometry***, where the 'sidewalls' are at $x = \pm L_x$ and $y = \pm L_y$ with L_x and L_y much larger than d. The influence of the sidewalls is therefore, in a first approximation, negligible: this will allow the use of the mathematically interesting *'periodic boundary conditions'*, as it will be explained at the beginning of section 1.2.1.
Finally, note that a RBT cell can be seen as a simplistic model of the problem of heating a room by the soil.

1.1.2 Oberbeck - Boussinesq approximations and equations

We assume the ***Oberbeck - Boussinesq approximation*** that states that the density of the fluid depends on its temperature according to

$$\boxed{\rho \;=\; \rho_0\,[1-\alpha(T-T_0)]} \tag{1.3}$$

with ρ_0 the reference density, T_0 the reference temperature, α the thermal expansion coefficient. Thus, the fluid is assumed to be only ***weakly compressible***: the variations of the density are supposed to be small, and noticeable only in the buoyancy term in the Navier-Stokes equation. Consequently, the Oberbeck - Boussinesq form of the mass-conservation, Navier-Stokes and heat equations reads

$$\mathrm{div}\mathbf{v} \;=\; 0\;, \tag{1.4}$$

$$\frac{d\mathbf{v}}{dt} \;=\; \partial_t\mathbf{v} \;+\; (\mathbf{v}\cdot\boldsymbol{\nabla})\mathbf{v} \;=\; -\,\alpha T\,\mathbf{g} \;-\; \boldsymbol{\nabla}p' \;+\; \nu\boldsymbol{\Delta}\mathbf{v}\;, \tag{1.5}$$

$$\frac{dT}{dt} \;=\; \partial_t T \;+\; \mathbf{v}\cdot\boldsymbol{\nabla}T \;=\; \kappa\Delta T\;, \tag{1.6}$$

with ν the kinematic viscosity of the fluid, κ its heat diffusivity. The 'pressure' is a modified one, hence the notation p'.
These equations always admit a ***static solution***, that corresponds to a ***conduction state*** and satisfies the isothermal boundary conditions:

$$\boxed{\mathbf{v} \;=\; \mathbf{0}\;,\quad T \;=\; T_0 \;-\; \delta T\frac{z}{d} \quad \text{with} \quad \delta T \;=\; T_2-T_1}\;. \tag{1.7}$$

This confirms that convection can only set in through an ***instability*** of this static solution.
We introduce dimensionless equations with

$$\text{the thickness } d \text{ as the unit of length,} \tag{1.8a}$$

$$\text{the heat diffusion time } \;\tau_{\text{therm}} \;=\; d^2/\kappa \;\text{ as the unit of time,} \tag{1.8b}$$

$$V \;=\; d/\tau_{\text{therm}} \;=\; \kappa/d \;\text{ as the unit of velocity,} \tag{1.8c}$$

$$\delta T \;\text{ as the unit of temperature.} \tag{1.8d}$$

We also introduce a ***dimensionless perturbation of temperature*** θ, such that the dimensionless temperature

$$\boxed{T' \;=\; T_0' \;-\; z' \;+\; \theta}\;. \tag{1.9}$$

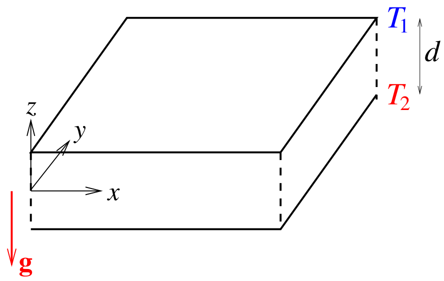

Fig. 1.1 : The ***Rayleigh-Bénard Thermoconvection*** system. A layer of fluid is sandwiched between two horizontal, isothermal plates, with $T_2 > T_1$. The lateral boundaries are only sketched because we consider the case of an ***extended geometry***.

Dropping the primes for the dimensionless quantities, we get the ***dimensionless Oberbeck - Boussinesq equations***

$$\mathrm{div}\mathbf{v} \;=\; 0 \;, \tag{1.10}$$

$$P^{-1}\frac{d\mathbf{v}}{dt} \;=\; R\theta\,\mathbf{e}_z \;-\; \boldsymbol{\nabla}p \;+\; \boldsymbol{\Delta}\mathbf{v} \;, \tag{1.11}$$

$$\frac{d\theta}{dt} \;=\; \Delta\theta \;+\; v_z \;, \tag{1.12}$$

with

the ***Rayleigh number*** $\boxed{R \;=\; \alpha\delta T g d^3/(\kappa\nu)}$ and the ***Prandtl number*** $\boxed{P \;=\; \nu/\kappa}$. (1.13)

Because of the ***isotropy of the problem in the horizontal plane*** we may focus on 2D xz solutions

$$\mathbf{v} \;=\; v_x(x,z,t)\;\mathbf{e}_x \;+\; v_z(x,z,t)\;\mathbf{e}_z \;, \quad \theta \;=\; \theta(x,z,t) \;. \tag{1.14}$$

Thus the mass-conservation equation (1.10) can be solved conveniently by using a ***streamfunction*** ψ such that

$$\boxed{\mathbf{v} \;=\; \mathbf{curl}(\psi\;\mathbf{e}_y) \;=\; (\boldsymbol{\nabla}\psi)\times\mathbf{e}_y \;=\; -(\partial_z\psi)\;\mathbf{e}_x \;+\; (\partial_x\psi)\;\mathbf{e}_z} \;. \tag{1.15}$$

Moreover, the pressure can be eliminated by solving, instead of the Navier-Stokes equation (1.11), the ***vorticity equation***, which reduces to its component in the y direction,

$$P^{-1}\partial_t(-\Delta\psi) \;+\; P^{-1}\big[\partial_z\big(\mathbf{v}\cdot\boldsymbol{\nabla}v_x\big) - \partial_x\big(\mathbf{v}\cdot\boldsymbol{\nabla}v_z\big)\big] \;=\; -R\partial_x\theta \;+\; \Delta(-\Delta\psi) \;. \tag{1.16}$$

To put the equations (1.16) and (1.12) under a 'matrix form', we introduce the ***local state vector***

$$V \;=\; \begin{bmatrix}\psi\\ \theta\end{bmatrix} \quad \text{also denoted} \quad (\psi,\;\theta) \;. \tag{1.17}$$

It fulfills

$$\boxed{D\cdot\partial_t V \;=\; L_R\cdot V \;+\; N_2(V,V)} \tag{1.18}$$

with D, L_R the ***linear***, N_2 the ***nonlinear differential operators*** defined by[1]

$$[D\cdot\partial_t V]_\psi \;=\; P^{-1}(-\Delta\partial_t\psi) \;, \quad [L_R\cdot V]_\psi \;=\; -R\partial_x\theta \;+\; \Delta(-\Delta\psi) \;, \tag{1.19a}$$

$$[N_2(V,V)]_\psi \;=\; P^{-1}\big[\partial_x\big(\mathbf{v}\cdot\boldsymbol{\nabla}v_z\big) - \partial_z\big(\mathbf{v}\cdot\boldsymbol{\nabla}v_x\big)\big] \;, \tag{1.19b}$$

$$[D\cdot\partial_t V]_\theta \;=\; \partial_t\theta \;, \quad [L_R\cdot V]_\theta \;=\; \Delta\theta \;+\; v_z \;, \quad [N_2(V,V)]_\theta \;=\; -\mathbf{v}\cdot\boldsymbol{\nabla}\theta \;. \tag{1.19c}$$

[1] The indices ψ or θ after the brackets in equations (1.19) refer to the 1^{st} or 2^{d} component of the vector inside the brackets.

1.1.3 Boundary conditions at the horizontal plates

The boundary conditions on θ describe ***isothermal boundaries***:

$$\theta = 0 \quad \text{if} \quad z = \pm 1/2 \ . \tag{1.20}$$

The most physical boundary conditions on ψ describe ***no-slip boundaries***:

$$v_x = v_z = 0 \quad \Longleftrightarrow \quad \partial_x \psi = \partial_z \psi = 0 \quad \text{if} \quad z = \pm 1/2 \ . \tag{1.21}$$

However, with such boundary conditions even the linear problem requires numerical computations (exercise 1.10), whereas more 'idealistic' conditions of slip boundaries without shear stress permit analytical calculations, and will therefore be chosen in a first approach. These ***'slip boundary conditions'***, also denoted ***'stress-free boundary conditions'***, read

$$v_z = 0 \quad \text{and} \quad S_{xz} = \ 0 \quad \text{if} \quad z = \pm 1/2 \ , \tag{1.22}$$

with S_{xz} the xz component of the rate-of-strain tensor (0.5) that yields the tangential stresses at the boundaries

$$S_{xz} \ = \ \frac{1}{2}(\partial_z v_x + \partial_x v_z) \ . \tag{1.23}$$

Thus, the conditions (1.22) reduce to

$$v_z = 0 \quad \text{and} \quad \partial_z v_x = \ 0 \quad \Longleftrightarrow \quad \partial_x \psi = \partial_z^2 \psi = 0 \quad \text{if} \quad z = \pm 1/2 \ . \tag{1.24}$$

1.2 Linear stability analysis of slip RBT

Since the solution $V = (0, 0)$ or '$V = 0$' of (1.18) always exists, the problem of the onset of convection can be attacked with a ***linear stability analysis***, here, a ***'temporal'*** stability analysis[2].

1.2.1 Linear stability analysis: general modal approach

Generally, in such an analysis the vector V is supposed to be small, hence a nonlinear problem of the form (1.18) is replaced by its linearized version, the linear problem

$$\boxed{D \cdot \partial_t V \ = \ L_R \cdot V} \ . \tag{1.25}$$

This problem is solved using a ***complex modal analysis***, i.e., by a ***superposition*** of ***linear eigenmodes*** or ***normal modes*** $V_1(\mathbf{q})$ that depends on numbers $\mathbf{q}$, on R and on the other parameters of the problem (this dependence is not recalled), and fulfill

$$\boxed{\sigma(\mathbf{q}, R) \ D \cdot V_1(\mathbf{q}) \ = \ L_R \cdot V_1(\mathbf{q})} \ . \tag{1.26}$$

This equation (1.26) corresponds to a ***generalized eigenvalue problem***[3]. There $\sigma(\mathbf{q}, R) \in \mathbb{C}$ is the ***temporal eigenvalue***, since the solution of (1.25) with the initial condition

$$V(t = 0) \ = \ A_0 \ V_1(\mathbf{q}) \tag{1.27}$$

[2] We will see in section 2.4 that in open flows a ***'spatial'*** stability analysis may be equally relevant.

[3] Because D is not identity; in the exceptional cases where D is identity, one recovers a ('simple') ***eigenvalue problem***.

is

$$V(t) \;=\; A_0 \;\; e^{\sigma(\mathbf{q},R)\;t}\; V_1(\mathbf{q})\;.$$

For systems that are locally invariant by translations $x \mapsto x + \ell$, one usually adopts simple conditions of periodicity under $x \mapsto x + L$ (‘*periodic boundary conditions*’) that may be relevant for real systems of finite but ‘large’ size in the x direction, with the belief that these transversal boundaries do not strongly influence the behaviour of the system ‘far from the boundaries’ (‘*extended geometry*’). Therefore, in a ‘Fourier’ approach, the modes $V_1(\mathbf{q})$ are Fourier modes

$$V_1(\mathbf{q}) \;=\; \widetilde{V}_1(k, \mathbf{q}') \;\; e^{ikx} \tag{1.28}$$

with k the ***wavenumber*** in the x-direction[4] and $\mathbf{q}'$ the other numbers that label the modes. Then the solution of (1.25) with the initial condition (1.27) reads

$$V(t) \;=\; A_0 \;\; e^{ikx \;+\; \sigma(\mathbf{q},R)\;t}\; \widetilde{V}_1(k, \mathbf{q}') \;=\; A_0 \;\; e^{i(kx+\sigma_i t)} \;\; e^{\sigma_r t}\; \widetilde{V}_1(k, \mathbf{q}') \tag{1.29}$$

where we have used a decomposition of $\sigma(\mathbf{q}, R)$ in real and imaginary parts,

$$\sigma(\mathbf{q}, R) \;=\; \sigma_r(\mathbf{q}, R) + i\sigma_i(\mathbf{q}, R)\;. \tag{1.30}$$

Therefore, we distinguish three cases, depending on the sign of $\sigma_r(\mathbf{q}, R)$:

- if $\sigma_r > 0$, the mode is ***amplified***, with the ***growth rate*** σ_r ;
- if $\sigma_r = 0$, the mode is ***neutral*** ;
- if $\sigma_r < 0$, the mode is ***damped***, with the ***damping rate*** $-\sigma_r$.

Assuming that $k > 0$, we also distinguish three cases, depending on the sign of $\sigma_i(\mathbf{q}, R)$:

- if $\sigma_i > 0$, the mode is ***oscillating***, it is a ***left-traveling wave***, with an ***angular frequency*** $\omega = \sigma_i$ and a ***phase velocity*** $c = \omega/k$;
- if $\sigma_i = 0$, the mode is ***‘non-oscillating’*** ;
- if $\sigma_i < 0$, the mode is ***oscillating***, it is a ***right-traveling wave***, with an ***angular frequency*** $\omega = -\sigma_i$ and a ***phase velocity*** $c = \omega/k$.

The trivial solution $V = 0$ of (1.25) is ***stable*** if no amplified mode exist - ***unstable*** as soon as one amplified mode exists.

1.2.2 Linear stability analysis of slip RBT

We now perform the linear stability analysis of slip RBT, in three steps - three exercises.

[4] An integer multiple of $2\pi/L$. If L is large, the discrete set of the possible values of k is almost $\mathbb{R}$.

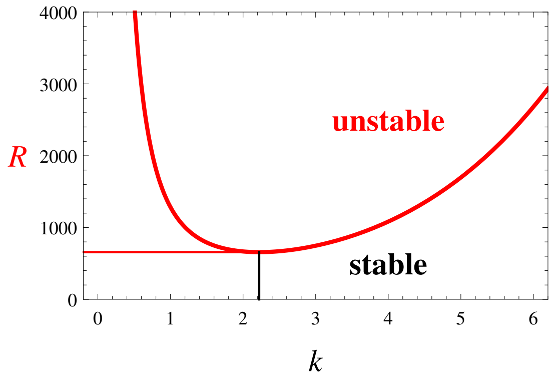

Fig. 1.2 : DIY ! In the wavenumber - Rayleigh number plane, neutral curve of slip RBT. The straight lines mark the critical wavenumber and Rayleigh number.

Exercise 1.1 ***Linear stability analysis of slip RBT - Most relevant modes***

Check that modes of the form

$$V_1(k,\pm) \;=\; (\Psi,\;\Theta)\;\exp(ikx)\;\cos(\pi z) \tag{1.31}$$

with $k > 0$, Ψ and Θ two complex numbers, are eigenmodes of the problem (1.25) for slip RBT, provided that the ratio Ψ/Θ assumes a precise value, and that $\sigma = \sigma(k,\pm,R)$ fulfills a characteristic equation of degree 2. Show that this characteristic equation reads

$$\sigma^2 \;+\; (1+P)D_1\,\sigma \;+\; P(D_1^3 - Rk^2)/D_1 \;\;=\; 0 \quad \text{with} \quad D_1 = k^2+\pi^2\ . \tag{1.32}$$

Check that this equation has two real roots $\sigma_\pm$, which correspond to a mode $V_1(k,-)$ that is always damped, and a mode $V_1(k,+)$ that may becomes amplified. For this purpose, calculate the discriminant of this equation and the symmetric functions of its roots

$$\sigma_+ \;+\; \sigma_- \;\;=\;\; -(1+P)D_1 \tag{1.33a}$$

$$\sigma_+\;\sigma_- \;\;=\;\; P(D_1^3 - Rk^2)/D_1 \tag{1.33b}$$

and study their signs. Thus show that $V_1(k,+)$ becomes amplified if the Rayleigh number exceeds a ***neutral value***

$$R_0(k) \;=\; \frac{(k^2+\pi^2)^3}{k^2}\ . \tag{1.34}$$

Plot the corresponding curve on figure 1.2, and identify the ***critical Rayleigh number***

$$R_c \;=\; 27\pi^4/4 \;=\; 657.5 \tag{1.35}$$

above which the conduction solution looses its stability. The first amplified mode, the so-called ***critical mode***, has an x-wavenumber which is the ***critical wavenumber***

$$k_c \;=\; \pi/\sqrt{2} \;=\; 2.22\ . \tag{1.36}$$

This corresponds to a ***critical wavelength***

$$\lambda_c \;=\; 2\pi/k_c \;=\; 2\sqrt{2} \;=\; 2.83\ . \tag{1.37}$$

The precise form of the complex ***critical mode***

$$V_{1c} \;=\; (-3i\pi/\sqrt{2},\;1)\;\exp(ik_c x)\;\cos(\pi z) \tag{1.38}$$

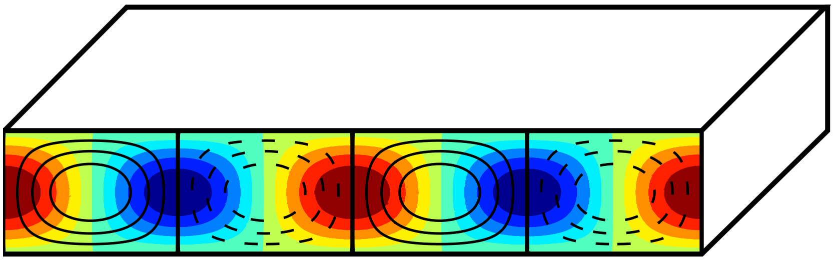

Fig. 1.3 : DIY ! In a vertical slice of an extended RBT cell, sketch of the streamlines and isotherms of the 'pure' critical rolls defined by equation (1.39). Two wavelengths (1.37) are shown.

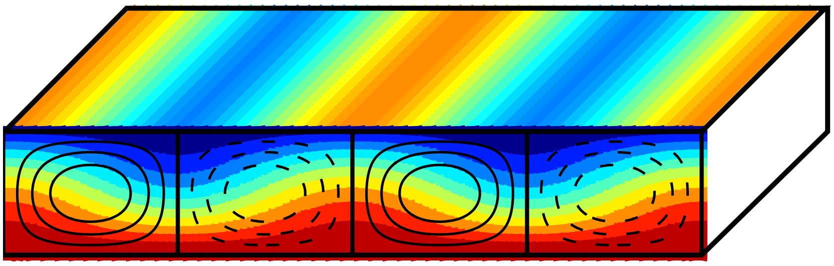

Fig. 1.4 : DIY ! In a vertical slice of an extended RBT cell, sketch of the streamlines and isotherms of a realistic solution which includes the basic profile of temperature and a perturbation corresponding to the critical rolls defined by equation (1.39). On the upper plate, sketch of the temperature field averaged over z.

leads to a real critical mode

$$V_{1r} \;=\; AV_{1c} + c.c. \;=\; A(3\sqrt{2}\pi \;\sin(k_c x),\; 2\cos(k_c x))\;\cos(\pi z)\;. \tag{1.39}$$

Using preferentially Mathematica, with the command `ContourPlot`, plot the streamlines and isotherms of this pure mode in the layer in figure 1.3, and explain the ***instability loop*** that amplifies this mode.
Finally, by adding the mode (1.39), with a small amplitude, to the basic state, i.e., remembering equation (1.9), plot the streamlines and isotherms in the layer of a realistic structure in figure 1.4, and sketch also, above the layer, the temperature field averaged over z. Explain the terms ***'roll patterns'*** and ***'patterning bifurcation'***.

All this is confirmed by experiments, such as the ones of Hu *et al.* (1993), which display nice roll patterns. See figure 1.9 ; note, however, that the boundary conditions in the experiments are 'no-slip' instead of 'stress-free'.

Exercise 1.2 ***General linear stability analysis of slip RBT***

To perform a general linear stability analysis of the problem (1.18) with the boundary conditions (1.20) and (1.24), it is more convenient to use another frame $\mathrm{O}xyz'$ where the layer is located between $z' = 0$ (bottom plate) and $z' = 1$ (top plate), i.e., to use $z' = z + 1/2$. In this exercise, we note z instead of z', i.e. $z \in \;]0, 1[$.

1 Calculate ***systematically*** all x-homogeneous normal modes, that do not depend on x, and have been disregarded in exercise 1.1. Show that they are indeed 'irrelevant'.

Indications:

Observe that the heat and vorticity equations are decoupled.
First, solve the heat equation. Search solutions of the form $\theta = a_+ \ e^{rz} + a_- \ e^{-rz}$. Establish a link between r and the temporal eigenvalue σ. With the boundary conditions, obtain an homogeneous system on (a_+, a_-). Explain why the determinant of this system must vanish. From this condition, obtain the values of σ, and the form of θ...
Second, observe that ψ'' obeys an equation similar to the heat equation...

2 Focus now on x-dependent solutions. In exercise 1.1, we have calculated only one family of Fourier normal modes,

$$V_1(k, \pm) \ = \ (\Psi(k, \pm), \ \Theta(k, \pm)) \ \exp(ikx) \ \sin(\pi z) \ , \tag{1.40}$$

with $k \neq 0$ the x-wavenumber. Thus, the fact that an initial condition

$$V(t = 0) \ = \ (\psi(t = 0), \ \theta(t = 0))$$

can be decomposed on the basis of all normal modes

$$V(t = 0) \ = \ \sum_{\mathbf{q}} A(\mathbf{q}) V_1(\mathbf{q})$$

is unclear, as is also the precise meaning of $\mathbf{q}$, the labels that index all normal modes.
For the sake of simplicity, we consider periodic boundary conditions in the x direction, under $x \mapsto x + L$. Hence exponential Fourier series can be used to analyse the x dependence, i.e. $\mathbf{q}$ contains generally the x-wavenumber k such that

$$V_1(\mathbf{q}) \ = \ V_1(k, \mathbf{q}') \ = \ V_1(z; k, \mathbf{q}') \ \exp(ikx)$$

with $k \in \mathbb{K}$, $\mathbb{K} = (2\pi/L)\mathbb{Z}$, $\mathbf{q}'$ other labels that have to be identified.

Show that modes

$$V_1(k, \pm, n) \ = \ (\Psi(k, \pm, n), \ \Theta(k, \pm, n)) \ \exp(ikx) \ \sin(n\pi z) \tag{1.41}$$

with $n \in \mathbb{N}^*$ are also normal modes, provided that the ratio Ψ/Θ is set, and σ takes particular values determined by a characteristic equation. Check that for given k and n, there are indeed two modes $+$ and $-$ and two eigenvalues $\sigma(k, \pm, n)$. Check that with $n = 1$ you recover the modes (1.40) and their corresponding eigenvalues. Check that the most relevant modes are indeed the modes with $n = 1$.

Comments:

From a mathematical point of view, the fact that any initial condition can be written as

$$V(t = 0) \ = \ \sum_{k \in \mathbb{K}} \ \sum_{s = \pm} \ \sum_{n \in \mathbb{N}^*} A(k, s, n) \ V_1(k, s, n) \tag{1.42}$$

results from a development in exponential Fourier series of x, trigonometric Fourier series of z, and from the fact that, for given k and n, $(\Psi(k, +, n), \ \Theta(k, +, n))$ and $(\Psi(k, -, n), \ \Theta(k, -, n))$ form a basis of $\mathbb{C}^2$.
Coming back to $z \in \ ]-1/2, 1/2[$, the following symmetry property can be shown: all normal modes are *either* even *or* odd under the midplane reflection symmetry $z \mapsto -z$.

Exercise 1.3 ***Characteristic time of the instability***

Let us define the (dimensionless) ***characteristic time of the instability*** as the real positive number τ_0 such that the critical eigenvalue, $\sigma(k_c, +, 1, R, P)$ if one recalls all dependencies, σ_+ if one uses concise notations, behaves near onset as

$$\sigma_+ \;=\; \frac{1}{\tau_0}\frac{R-R_c}{R_c} \;+\; o(R-R_c) \;. \tag{1.43}$$

To further simplify the notations, we define the ***'bifurcation parameter'***

$$\boxed{\epsilon \;=\; R/R_c - 1} \tag{1.44}$$

which is assumed to be small here[5]. Thus τ_0 is defined by the equation

$$\boxed{\sigma_+ \;=\; \epsilon/\tau_0 \;+\; o(\epsilon)} \tag{1.45}$$

fulfilled as $\epsilon \to 0$. Noting that the other root of the characteristic equation (1.32) behaves in the same limit as

$$\sigma_- \;=\; -\,\sigma_1 \;+\; o(\epsilon) \;,$$

using the symmetric functions of the roots (1.33), calculate

$$\tau_0 \;=\; \frac{2}{3\pi^2}\,(1+P^{-1}) \quad . \tag{1.46}$$

Give also the characteristic time of the instability in physical units,

$$\tau_0^{\text{dimensional}} \;=\; \frac{2d^2}{3\pi^2\kappa}\,(1+P^{-1}) \;. \tag{1.47}$$

Give approximate formulas for $\tau_0^{\text{dimensional}}$ in the limits $P \gg 1$ and $P \ll 1$. Give a physical interpretation of these regimes and of the formulas for $\tau_0^{\text{dimensional}}$ by considering also (and comparing with) the heat diffusion time τ_{therm} (1.8*b*) and the viscous diffusion time

$$\tau_{\text{visc}} \;=\; d^2/\nu \;. \tag{1.48}$$

1.3 The linear modes basis - The adjoint problem & adjoint modes

In this section 1.3 and in the forthcoming section 1.4, we consider, as the fluid domain, a box with periodic boundary conditions under $x \mapsto x + \lambda_c$. Consequently, the wavenumber $k \;\in\; \mathbb{K}$ with $\mathbb{K} \;=\; k_c\mathbb{Z}$. Hence we can label the normal modes with $\mathbf{q} \;=\; (k,s,n) \in\; \mathbb{K}\times\{+,-\}\times\mathbb{N}^*$, and a general field can always be written as a superposition of normal modes,

$$V \;=\; \sum_{k\in\mathbb{K}}\;\sum_{s=\pm}\;\sum_{n\in\mathbb{N}^*} A(k,s,n)\;V_1(k,s,n) = \;\sum_{\mathbf{q}} A(\mathbf{q})\;V_1(\mathbf{q}) \;. \tag{1.49}$$

It is important to be able to calculate systematically the 'amplitudes' $A(\mathbf{q})$. For this purpose, we introduce (generally, the technique is not specific to RBT) the ***adjoint problem*** and ***adjoint modes*** as follows.

[5] And also in the weakly nonlinear analysis of section 1.4.

1.3.1 Adjoint problem & adjoint modes: general principles

- We first introduce the ***Hermitian inner product***

$$\langle V,\ U\rangle \ = \ \int_{x=0}^{\lambda_c}\int_{z=-1/2}^{1/2} V(x,z)\cdot U^*(x,z)\ \frac{dx}{\lambda_c}\ dz\ . \tag{1.50}$$

- We then define the ***adjoint operators*** $D^\dagger$ and $L^\dagger$ such that

$$\forall V,U,\quad \langle D\cdot V,\ U\rangle \ = \ \Big\langle V,\ D^\dagger\cdot U\Big\rangle \quad \text{and} \quad \langle L\cdot V,\ U\rangle \ = \ \Big\langle V,\ L^\dagger\cdot U\Big\rangle\ , \tag{1.51}$$

  V and U satisfying the boundary conditions of the problem.

- We assume[6] that the ***adjoint eigenproblem***

$$\sigma^* D^\dagger\cdot U \ = \ L^\dagger\cdot U \tag{1.52}$$

  has eigenvalues σ^* that are the complex conjugates of the ones σ of the direct eigenproblem.

- Therefore to each direct mode $V_1(\mathbf{q})$ of eigenvalue $\sigma(\mathbf{q})$ there correspond ***adjoint modes*** $U_1(\mathbf{q})$ of eigenvalue $\sigma^*(\mathbf{q})$ with the same wavenumber k.

- If k in $\mathbf{q}\ \neq k'$ in $\mathbf{q}'$ then

$$\big\langle D\cdot V_1(\mathbf{q}),\ U_1(\mathbf{q}')\big\rangle \ = \ \big\langle L\cdot V_1(\mathbf{q}),\ U_1(\mathbf{q}')\big\rangle \ = \ 0\ . \tag{1.53}$$

- For $\mathbf{q}$ with the same wavenumber k, one has usually non degenerate eigenvalues:

$$\text{if } k \text{ in } \mathbf{q} \ = \ k \text{ in } \mathbf{q}' \ \text{ but }\ \mathbf{q}\neq\mathbf{q}'\ ,\quad \sigma=\sigma(\mathbf{q})\ \neq\ \sigma'=\sigma(\mathbf{q}')\ . \tag{1.54}$$

- Consequently one can show that

$$\mathbf{q}\neq\mathbf{q}' \quad\Longrightarrow\quad \big\langle D\cdot V_1(\mathbf{q}),\ U_1(\mathbf{q}')\big\rangle \ = \ \big\langle L\cdot V_1(\mathbf{q}),\ U_1(\mathbf{q}')\big\rangle \ = \ 0\ . \tag{1.55}$$

- Normalizing the adjoint modes such that

$$\forall\mathbf{q}\ ,\quad \langle D\cdot V_1(\mathbf{q}),\ U_1(\mathbf{q})\rangle \ = \ 1\ , \tag{1.56}$$

  we find that the amplitudes in (1.49) are given by

$$\boxed{A(\mathbf{q}) \ = \ \langle D\cdot V,\ U_1(\mathbf{q})\rangle}\ . \tag{1.57}$$

Physical meaning of an adjoint mode: ‘receptivity function’

In order to analyze the physics behind adjoint modes, let us consider briefly a (linearized) ***forcing problem***

$$D\cdot\partial_t V \ = \ L\cdot V \ + \ F \tag{1.58}$$

with $F = F(x,z,t)$ the ***forcing terms***, corresponding to source terms in the vorticity and heat equation. Seeking solutions of the form

$$V \ = \ \sum_{\mathbf{q}} A(\mathbf{q},t)\ V_1(\mathbf{q})\ ,$$

[6] This is very often the case, at least this works for RBT... and this will work for PPF, see chapter 2...

we obtain

$$\sum_{\mathbf{q}} \frac{dA}{dt}(\mathbf{q},t)\ D\cdot V_1(\mathbf{q}) \ = \ \sum_{\mathbf{q}} \sigma(\mathbf{q})A(\mathbf{q},t)\ D\cdot V_1(\mathbf{q}) \ + \ F\ .$$

With a projection onto $U_1(\mathbf{q})$, we find the *'amplitude equations'*

$$\frac{dA}{dt}(\mathbf{q},t) \ = \ \sigma(\mathbf{q})A(\mathbf{q},t) \ + \ \langle F,\ U_1(\mathbf{q})\rangle$$

Hence the ***forcing term*** in the equation for $A(\mathbf{q},t)$ reads

$$\langle F,\ U_1(\mathbf{q})\rangle \ = \ \int_{x=0}^{\lambda_c}\int_{z=-1/2}^{1/2} F(x,z,t)\cdot U_1^*(\mathbf{q};x,z)\ \frac{dx}{\lambda_c}\ dz\ .$$

Thus the components of $U_1(\mathbf{q})$ measure the ***'receptivity'*** of the mode $V_1(\mathbf{q})$ to ***perturbation***.

1.3.2 Adjoint problem & adjoint modes in slip RBT

Exercise 1.4 ***Adjoint problem in slip RBT***

Denoting $U = (\psi_a,\theta_a)$, calculate analytically the adjoint problem of the RBT linearized problem, with slip boundaries. Focus on the case of Fourier modes in x, of x-wavenumber $k \neq 0$.

Indications:

Start with the calculation of $D^\dagger$. It will be useful to use ***recursive integrations by parts***: if u and v are functions of z of class C^n, one has

$$\int uv^{(n)}\ dz \ = \ \left[uv^{(n-1)} \ - \ u'v^{(n-2)} \ + \ u''v^{(n-3)} \ + \ ... \ + \ (-1)^{n-1}u^{(n-1)}v\right] \ + \ (-1)^n\int u^{(n)}v\ dz$$

which can be explicited with the help of this table:

	Column A Derivatives of u	Column B Derivatives of v
$+$	u	$v^{(n)}$
$-$	$u^{(1)}$	$v^{(n-1)}$
	$\vdots$	$\vdots$
$(-1)^n$	$u^{(n)}$	v

and of this rule: pair the 1st entry of column A with the 2d entry of column B, the 2d entry of column A with the 3rd entry of column B, etc... with alternating signs (beginning with the positive sign)...

Solution:

$$D^\dagger \ = \ D\ , \quad [L_R^\dagger\cdot U]_\psi \ = \ -\Delta\Delta\psi_a \ - \ ik\theta_a\ , \quad [L_R^\dagger\cdot U]_\theta \ = \ \Delta\theta_a \ + \ Rik\psi_a\ . \tag{1.59}$$

Exercise 1.5 ***Adjoint critical mode in RBT with slip boundaries***

For $k = k_c = \pi/\sqrt{2}$, $R = R_c = 27\pi^4/4$, to the critical mode (1.38), check that there corresponds a neutral ***adjoint critical mode*** U_{1c} with the same dependence in x and z; calculate it with the normalization condition (1.56).

Solution:

$$U_{1c} \ = \ \frac{2}{1+P^{-1}}(-i2\sqrt{2}/(9\pi^3),\ 1)\ \exp(ik_cx)\ \cos(\pi z)\ . \tag{1.60}$$

1.4 Weakly nonlinear analysis of slip RBT

We recall that we consider, as the fluid domain, the periodic box described at the beginning of section 1.3. We seek, for R close to R_c, i.e., for a ***bifurcation parameter***

$$\boxed{\epsilon \ = \ R/R_c - 1 \ \ll \ 1} \ , \tag{1.61}$$

an approximate solution of the nonlinear problem (1.18) of the form (1.49),

$$V \ = \ \sum_{\mathbf{q}} A(\mathbf{q},t) \ V_1(\mathbf{q}) \ . \tag{1.62}$$

Following Haken (1983) *'Long-living systems slave short-living systems'*, we distinguish

- ***active modes*** that correspond to $\mathbf{q} = \mathbf{q}_c = (k_c, +, 1)$ or $\mathbf{q}_c^* = (-k_c, +, 1)$ and are long-living

$$\sigma(\mathbf{q}, R) \ \sim \ \epsilon/\tau_0 \tag{1.63}$$

  with τ_0 the characteristic time of the instability calculated in exercise 1.3,

- from the ***passive modes*** that correspond to $\mathbf{q} \neq \mathbf{q}_c, \mathbf{q}_c^*$ and are short-living (rapidly damped)

$$\sigma(\mathbf{q}, R) \ < \ \sigma_1 \ < \ 0 \ . \tag{1.64}$$

We assume that, possibly after a short transient, the active modes dictate the dynamics. The amplitudes are assumed to be ***slowly varying***

$$\forall \mathbf{q} \ , \quad \frac{dA}{dt}(\mathbf{q},t) \ = \ O(\epsilon \ A(\mathbf{q},t)) \ . \tag{1.65}$$

Thus,

$$\boxed{V \ = \ V_a \ + \ V_\perp} \quad \text{with} \quad \boxed{V_a \ = \ A_{1c}V_{1c} \ + \ c.c.} \ \text{the } \textbf{\textit{active modes}}, \ \ V_a \ \ll \ 1 \ , \tag{1.66}$$

$$V_\perp \ = \ \sum_{\mathbf{q} \neq \mathbf{q}_c, \mathbf{q}_c^*} A(\mathbf{q},t) \ V_1(\mathbf{q}) \ \text{the } \textbf{\textit{passive modes}}, \ \ V_\perp \ \ll \ V_a \ . \tag{1.67}$$

In the amplitude equations for the passive modes,

$$\frac{dA}{dt}(\mathbf{q},t) \ = \ \sigma(\mathbf{q},R)A(\mathbf{q},t) \ + \ \sum_{\mathbf{q}_1}\sum_{\mathbf{q}_2} A(\mathbf{q}_1,t)A(\mathbf{q}_2,t) \, \langle N_2(V_1(\mathbf{q}_1), V_1(\mathbf{q}_2)), \ U_1(\mathbf{q})\rangle \ , \tag{1.68}$$

we may neglect dA/dt and consider that these modes are created by the active ones, through nonlinear effects. The passive modes are therefore obtained by ***quasistatic elimination***

$$0 \ = \ \sigma(\mathbf{q},R)A(\mathbf{q},t) \ + \sum_{\mathbf{q}_1 = \mathbf{q}_c, \mathbf{q}_c^*} \ \sum_{\mathbf{q}_2 = \mathbf{q}_c, \mathbf{q}_c^*} A(\mathbf{q}_1,t)A(\mathbf{q}_2,t) \, \langle N_2(V_1(\mathbf{q}_1), V_1(\mathbf{q}_2)), \ U_1(\mathbf{q})\rangle \tag{1.69}$$

which amounts here, for 'symmetry' reasons[7], to

$$0 \ = \ L_R \cdot V_\perp \ + \ N_2(V_a, V_a) \ . \tag{1.70}$$

[7] The nonlinear terms $N_2(V_a, V_a)$ may create only passive modes, of x-wavenumber 0 or $\pm 2k_c$ which are quite different from k_c.

Exercise 1.6 ***Quasistatic elimination of the passive mode in slip RBT***

In slip RBT, denoting $A = A_{1c}$ the amplitude of the critical mode, show with Mathematica that

$$[N_2(V_a, V_a)]_\psi = 0 \ , \quad [N_2(V_a, V_a)]_\theta = B \ \sin(2\pi z) \tag{1.71}$$

with B a real number,

$$B = 3\pi^3 A^2 \ . \tag{1.72}$$

Next, solve (1.70), showing that

$$\boxed{V_\perp = A^2 V_{20}} \quad \text{with} \quad V_{20} = (0, \ \Theta_2) = \left(0, \ \frac{3\pi}{4} \ \sin(2\pi z)\right) \ , \tag{1.73}$$

and explain the physics behind. For this purpose, complete the figures 1.5a and b.

Exercise 1.7 ***The passive mode in slip RBT first controls the Nusselt number***

Show that the passive mode that you have calculated controls the value of the Nusselt number

$$Nu = \frac{\Phi_{\text{heat with conduction \& convection}}}{\Phi_{\text{heat with conduction only}}} \tag{1.74}$$

with Φ_{heat} the average heat flux that goes from the hot bottom plate to the cold top plate.

Indication: you must prove that $Nu - 1 \propto A^2$.

Solution:

$$Nu - 1 = \frac{3\pi^2}{2} A^2 \ . \tag{1.75}$$

To determine A, we obtain, by projection of (1.18) onto the adjoint critical mode U_{1c} , the ***amplitude equation***

$$\frac{dA}{dt} = \frac{\epsilon}{\tau_0} A + \langle N_2(V, V), \ U_{1c} \rangle \ . \tag{1.76}$$

The nonlinear terms in $N_2(V, V)$ that have a nonzero projection on $U_1(\mathbf{q}_c)$ are ***'resonant'***.

Exercise 1.8 ***Resonant terms in slip RBT at order*** A^3

Compute with Mathematica the resonant terms in $N_2(V, V)$,

$$[N_2(V, V) \text{ resonant}]_\psi = 0 \ , \quad [N_2(V, V) \text{ resonant}]_\theta = -\frac{9\pi^4}{2} A^3 \ \cos(k_c x) \ \cos(\pi z) \ \cos(2\pi z) \ . \tag{1.77}$$

and explain their physics. For this purpose, complete the figure 1.5c.

Exercise 1.9 ***Saturation in slip RBT***

Show that $\langle N_2(V,V),\ U_{1c}\rangle = -gA^3$ and compute the ***saturation coefficient***

$$g \ = \ (9/8)\pi^4/(1+P^{-1}) \ . \tag{1.78}$$

Deduce from this and the knowledge of τ_0 an analytical expression of the Nusselt number in weakly nonlinear roll solutions,

$$Nu \ = \ 1+2\epsilon \ . \tag{1.79}$$

Comments:

'Solutions' refers to the stationary solutions (1.81) of the final amplitude equation (1.80). An important consequence of (1.79) is that $Nu - 1 \propto \delta T/(\delta T)_c - 1$, with $(\delta T)_c$ the critical value of the temperature difference. This is confirmed by experiments, see figure 1.10.

In conclusion, the ***amplitude equation*** (1.76) assumes the form

$$\boxed{\frac{dA}{dt} \ = \ \frac{\epsilon}{\tau_0}A \ - \ gA^3} \quad \text{with} \quad g \in \mathbb{R}^{+*} \ . \tag{1.80}$$

This is the generic equation of a ***supercritical pitchfork bifurcation***. As an exercise, calculate the stationary solutions, or 'fixed points', of equation (1.80):

$$\begin{aligned} \forall\epsilon \quad , \quad A \ &= \ 0 \ , \\ \forall\epsilon > 0 \quad , \quad A \ &= \ \pm\sqrt{\epsilon/(\tau_0 g)} \ . \end{aligned} \tag{1.81}$$

Then, construct in figure 1.6 the corresponding ***bifurcation diagram*** in the plane (ϵ, A) (bifurcation parameter, amplitude) plotting these solutions, that depend on ϵ, and arrows parallel to the A-axis indicating dA/dt. From the direction of these arrows, the trajectories of the dynamical system (1.80), which are line segments, can be immediately deduced. From this, the stability properties of the stationary solutions ensue... The result, figure 1.6, displays a *'pitchfork'*; moreover, the interesting non-vanishing stationary solutions exist only for $\epsilon > 0$ i.e. *above* (*'super'* in latin) onset; all this explain the name of the bifurcation...

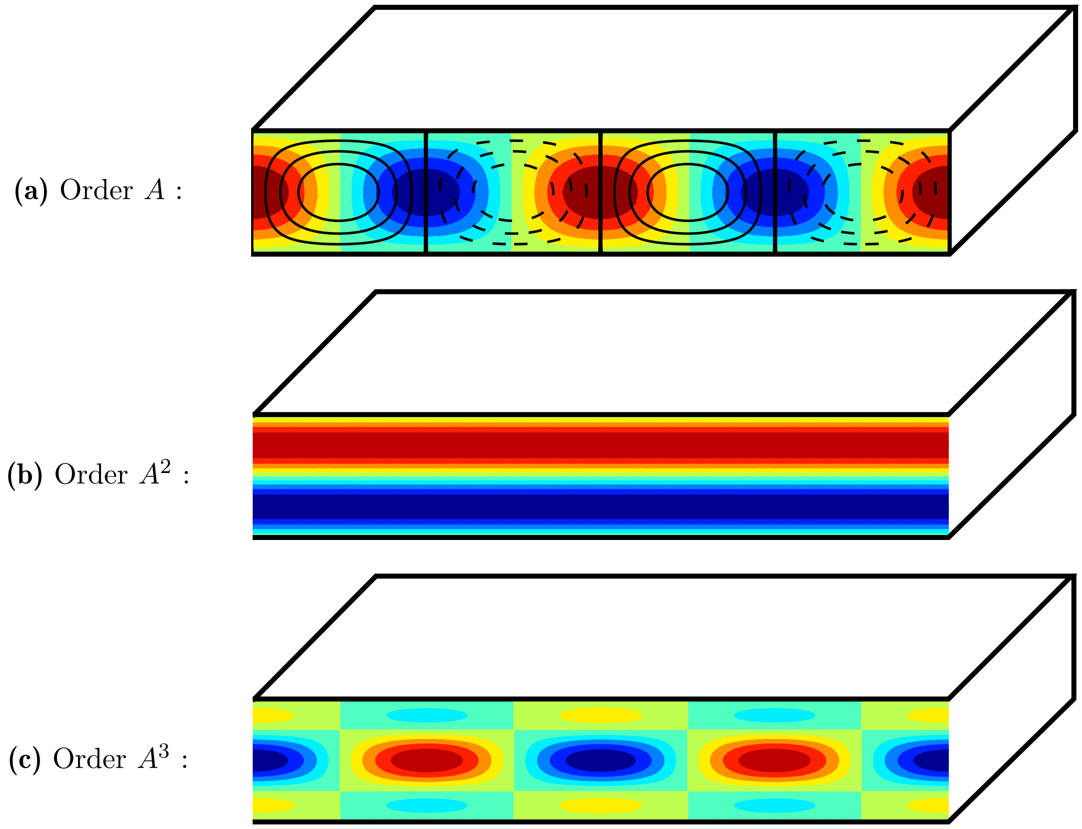

Fig. 1.5 : DIY ! **a:** Reproduction of the figure 1.3, the streamlines and isotherms of the 'pure' ***critical rolls*** defined by equation (1.39). **b:** The isotherms of the ***passive mode*** (1.73). **c:** The isotherms of the ***resonant term*** (1.77) in the heat equation. The comparison of the figures a and c shows the ***'saturation' effect*** of these resonant terms.

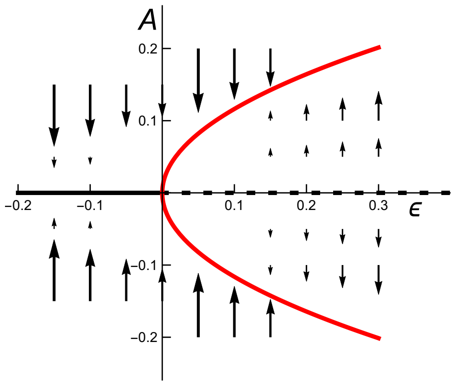

Fig. 1.6 : DIY ! ***Bifurcation diagram*** of the amplitude equation (1.80). The curves in black and grey (red online) show the stationary solutions, or 'fixed points'; with the continuous lines: stable solutions; with the dashed line: unstable solution. The arrows show vectors $(0,\ dA/dt)$ when $A(t)$ evolves according to equation (1.80), from an initial condition which is not a fixed point.

1.5 A glimpse at the Lorenz model and chaos

Considering the WNL solution found here,

$$V \;=\; V_a \;+\; V_\perp \;+\; h.o.t. \tag{1.82}$$

with

$$V_a \;=\; AV_{1c} \;+\; c.c. \;=\; A\,\left(3\sqrt{2}\pi\;\sin(k_c x),\; 2\cos(k_c x)\right)\;\cos(\pi z)\;, \tag{1.83}$$

$$V_\perp \;=\; A^2 V_{20} \;=\; A^2\,\left(0,\;\tfrac{3\pi}{4}\sin(2\pi z)\right)\;, \tag{1.84}$$

gave in 1963 to Edward Lorenz, an American mathematician and meteorologist, the idea to study thermoconvection flows containing the same contributions, but with 3 different amplitudes A, B and C,

$$\psi \;=\; A\;\sin(k_c x)\;\cos(\pi z)\;,\quad \theta \;=\; B\;\cos(k_c x)\;\cos(\pi z)\;+\;C\;\sin(2\pi z)\;. \tag{1.85}$$

By inserting this ansatz into the Oberbeck - Boussinesq equations, renormalizing time and the amplitudes $(A,\ B,\ C)$ to define new ones $(X,\ Y,\ Z)$, and disregarding a term in the heat equation, that cannot be balanced, he obtained the ***'Lorenz system'***

$$\begin{cases} P^{-1}\dot{X} &=& Y - X \\ \dot{Y} &=& rX - Y \;-\; XZ \\ \dot{Z} &=& -bZ \;+\; XY \end{cases} \tag{1.86}$$

with

$$r \;=\; R/R_c\;,\quad b \;=\; 8/3\;. \tag{1.87}$$

One can easily show that, for $r < 1$, the conduction solution

$$X \;=\; Y \;=\; Z \;=\; 0$$

is stable, whereas it becomes unstable if $r > 1$. Two new fixed points appear then, which correspond to weakly nonlinear thermoconvection rolls,

$$X \;=\; Y \;=\; \pm\sqrt{b(r-1)}\;,\quad Z \;=\; r-1\;. \tag{1.88}$$

This is quite coherent with the theory developped in sections 1.2 and 1.4.

By analyzing the stability of the roll solutions (1.88) in the framework of the model (1.86), one can show that, for Prandtl numbers $P > 11/3$, these solutions undergo at sufficiently large R (or r) a ***secondary oscillatory instability***, with temporal eigenvalues of the form $\pm i\omega$ with $\omega \in \mathbb{R}$ (see the problem 1.1). Numerical simulations show that this secondary instability leads to ***'chaos'***, i.e., a dynamic behaviour which displays a ***sensitive dependence on the initial condition***. This is demonstrated in the movie available on YouTube

Simple Model of the Lorenz Attractor
https://www.youtube.com/watch?v=FYE4JKAXSfY .

This movie shows, in the phase space $(X,\ Y,\ Z)$, how three nearby trajectories, which correspond first to 'oscillatory convection', suddenly diverge, and explore a 'large region' of phase space in a seemingly 'random' manner. The 'region' explored has a structure, it is in fact a ***'strange attractor'***. It can be thought of as a 'collection' of trajectories which are *all* unstable. This remarkable finding, published in Lorenz (1963), attracted the attentions of many scientists. Their work on this topics has lead to the development of the ***'theory of chaos'*** in the 1970s - 1980s, as illustrated by the treatise Bergé *et al.* (1984). The title of this treatise, *Order within Chaos: Towards a Deterministic Approach to Turbulence*, is meaningful... Indeed, the great relevance of continuum thermomechanics suggests that the randomness characteristic of Turbulence rests on a deterministic dynamics... Coming back to slip RBT, the Lorenz model has to be seen as a crude model, but the fact that, within this model, thermoconvection takes, after a secondary instability, the form of a weakly turbulent flow at high Rayleigh numbers, is an interesting lesson. We could ask what happens at quite large Rayleigh numbers in slip RBT, but, if we want to do good and quantitative physics, we have now to switch to the more realistic case of no-slip boundary conditions...

1.6 Numerical linear analysis of no-slip RBT

This exercise should better be taken up, in the course of the module, after the introduction to spectral methods that will be performed during the study of instabilities of open shear flows, see the problem 2.1.

Exercise 1.10 ***Numerical linear stability analysis of no-slip RBT with a spectral method***

We want to solve with Mathematica the ***linear Rayleigh-Bénard Thermoconvection*** (RBT) problem with ***no-slip*** boundary conditions, for a chosen numerical value of the Prandtl number P, e.g. $P = 1$, using a ***spectral method***. The ***normal Fourier modes***

$$V = V_1(k) = (\Psi(z),\ \Theta(z))\ \exp(ikx)\ , \tag{1.89}$$

with $k \neq 0$, are written, for the z-dependent parts, as a sum of simple polynomial functions:

$$\Psi(z) = \sum_{n=1}^{N_z} \Psi_n f_n(z) \qquad \text{with} \qquad f_n(z) = (1/2 - z)^2\ (z + 1/2)^2\ T_{2n-2}(2z)\ , \tag{1.90a}$$

$$\Theta(z) = \sum_{n=1}^{N_z} \Theta_n g_n(z) \qquad \text{with} \qquad g_n(z) = (1/2 - z)\ (z + 1/2)\ T_{2n-2}(2z)\ , \tag{1.90b}$$

T_n the n^{th} Chebyshev polynomial of the first kind, N_z the number of z-modes.

1.1 For a relevant value of N_z , plot a few functions f_n and g_n , the ***Gauss-Lobatto collocation points***

$$z_m = \cos[m\pi/(2N_z + 1)]/2 \qquad \text{for} \qquad m \in \{1, 2, \cdots, N_z\}\ , \tag{1.91}$$

and comment.

1.2 By evaluating the vorticity and heat equation at the Gauss-Lobatto collocation points, construct by blocks matrices that represent the operators D and L_R applied to the vector of the expansion coefficients $V_{\text{num}} = (\Psi_1, \cdots, \Psi_{N_z}, \Theta_1, \cdots, \Theta_{N_z})$. Note that n in equations (1.90) is a 'column index', m in equation (1.91) is a 'line index'. The structure of the main loops of your program should be:

```
Do[
   (* Vort. eq. : terms with Psi *)
   MatD[[m,n]]= ...
   MatL[[m,n]]= ...

   (* Vort. eq. : terms with Theta *)
   MatD[[m,Nz+n]]= 0 ;
   MatL[[m,Nz+n]]= ...

   (* Heat eq. : terms with Psi *)
   MatD[[Nz+m,n]]= 0 ;
   MatL[[Nz+m,n]]= ...

   (* Heat eq. : terms with Theta *)
   MatD[[Nz+m,Nz+n]]= ...
   MatL[[Nz+m,Nz+n]]= ...
  , {m,1,Nz}, {n,1,Nz}]
```

1.3 With the command `Eigenvalues`, find a numerical approximation of the temporal eigenvalues $\sigma(k, R, P = 1)$ for k fixed. Check the physical relevance of this 'spectrum'.

1.4 Sort these eigenvalues to find the most relevant one $\sigma_1(k, R, P = 1)$.

1.5 Define the ***neutral Rayleigh number*** $R_0(k)$ by finding a root of $\sigma_1(k, R, P = 1) = 0$. Plot the corresponding ***neutral curve***. Explain why this curve does not depend of the value of P chosen.

1.6 Find the ***critical parameters*** k_c and R_c by minimizing the neutral Rayleigh number.

1.7 Perform ***convergence tests*** by varying the number of modes N_z , saving your results at given N_z :

```
Put[{Rc,kc},"RckcNz"<>ToString[Nz]]
```

then comparing the results obtained with $N_z - 1$ vs N_z modes. For this purpose, load the previous file with the command

```
{Rcold,kcold} = Get["RckcNz"<>ToString[Nz-1]]
```

With the convergence criterion

```
converged = And[ Abs[Rc/Rcold-1]<0.001 , Abs[kc/kcold-1]<0.001 ]
```

determine the minimum number N_z of modes needed to 'converge'. Comment briefly, from a numerical point of view.

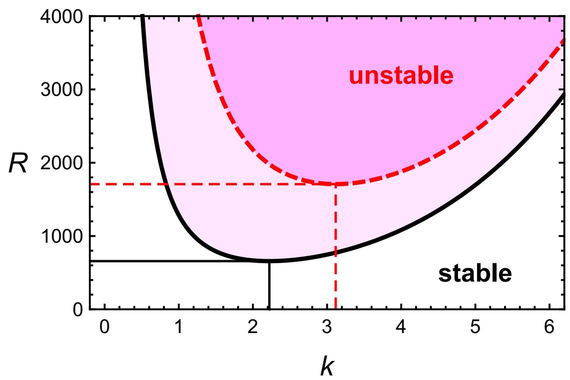

Fig. 1.7 : DIY ! In the wavenumber - Rayleigh number plane, the continuous line shows the ***neutral curve*** $R_0(k)$ ***of slip RBT***, the dashed line the ***neutral curve of no-slip RBT***. The straight lines show the critical parameters.

2.1 Using a notebook similar to the one used for question 1, but simplified, and made to be able to change the value of the Prandtl number P, create a function that computes the ***characteristic time of the instability*** $\tau_0(P)$ from

$$\sigma_1(k_c,\ R_c(1+\epsilon),\ P) \ = \ \frac{\epsilon}{\tau_0(P)} \ + \ O(\epsilon^2)\ . \tag{1.92}$$

For this purpose, first check, with a plot that shows the curve of $\sigma_1(k,\ R_c(1+\epsilon),\ P=1)$ vs ϵ and its tangent, that $\epsilon = 0.01$ is a relevant value to extract $\tau_0(P=1)$.

2.2 Construct a plot that demonstrates that the function $\tau_0(P)$ takes, at least in the interval $P \in [0.02, 100]$, the form

$$\tau_0(P) \ = \ a + bP^{-1}\ , \tag{1.93}$$

and compute a and b with at least two digits. Check the convergence of these computations.

Indication: it may help to use the commands `Fit` and `Coefficient`.

2.3 Comment briefly, from a physical point of view.

Elements of solution and comments:

As it is visible in figure 1.7, the critical Rayleigh number found,

$$R_c \ = \ 1708\ , \tag{1.94}$$

larger than the one (1.35) found with slip boundary conditions, demonstrates that the no-slip boundary conditions have, naturally, a ***stabilizing effect***. The critical wavelength,

$$\lambda_c \ = \ 2.01\ , \tag{1.95}$$

smaller than the one (1.37) found with slip boundary conditions, shows that the thermoconvection rolls require stronger gradients... and are almost 'squared'... One also finds that the characteristic time of the instability

$$\tau_0(P) \ = \ 0.0509 \ + \ 0.0260P^{-1} \tag{1.96}$$

has the same form of Prandtl-number dependence than in the slip case, compare with (1.46).

(a)

(b)

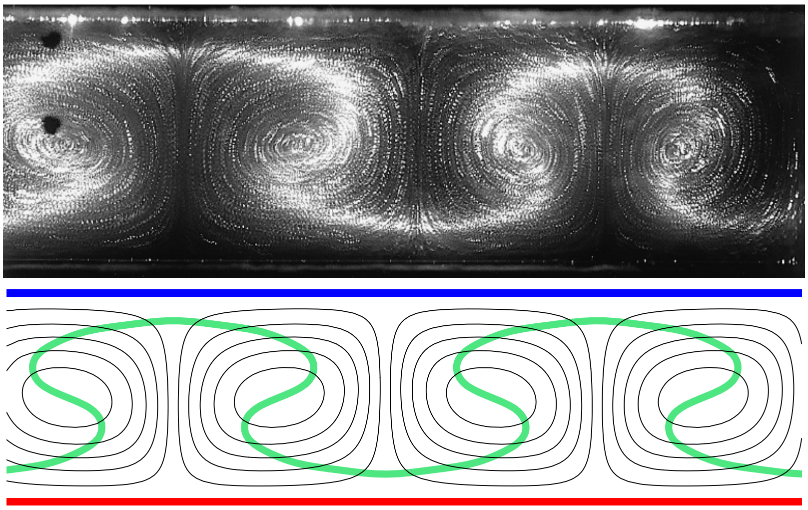

Fig. 1.8 : **a:** Experimental visualisation by Stasiek (1997) of ***thermoconvection rolls*** in a glycerol-filled cavity of 180 mm long, 60 mm wide and 30 mm high. The Prandtl number $P = 12.5\ 10^3$ and the Rayleigh number $R = 12\ 10^3$. A vertical 'plane' of thickness 2 - 3 mm in width is illuminated. Small drops, of diameter 50 - 80 μm, of thermochromic liquid crystals are dispersed in the glycerol. The photograph is taken with 8 flashes at a time interval of 6 seconds: the successive positions of the drops show the flow streamlines. Moreover, a selective reflection of light by the thermochromic liquid crystals shows in bright the isotherm corresponding roughly to the average T_0 of the temperatures of the horizontal boundaries. **b:** Thermoconvection rolls computed for the same values of P and R, and for the critical value of the wavenumber, with the spectral code of Plaut & Busse (2002). The thin black curves show the streamlines. The thick curve (gray in the printed, green in the PDF version) shows the isotherm at the mean temperature.

1.7 Short review of no-slip RBT

A ***weakly nonlinear analysis*** may be performed numerically, but with care to explicit the Prandtl number dependence of the solutions[8]. Thus, for instance, Schlüter *et al.* (1965) showed that the Nusselt number is given, in the weakly nonlinear regime, by

$$Nu \ = \ 1 + (0.699 \ + \ 0.00472 P^{-1} \ + \ 0.00832 P^{-2})^{-1} \epsilon \ + \ O(\epsilon^2) \ . \tag{1.97}$$

There is a strong Prandtl-number dependence, especially, as $P \to 0$, which is not at all present in the slip case: compare with equation (1.79). This illustrates the fact that nonlinear properties of a model are much more sensitive to the boundary conditions than linear properties... ***Strongly nonlinear computations*** may also be performed, for instance, with spectral methods. This is illustrated in figure 1.8, where the good agreement between the experiments (figure 1.8a) and the strongly nonlinear computations (figure 1.8b) proves the relevance of the Oberbeck - Boussinesq approximation and equations.

Other ***experimental results in extended geometry***, that confirm the bifurcation to rolls in no-slip RBT, are presented for instance in Hu *et al.* (1993). Their cylindrical setup is shown in figure 1.9a : RBT in CO_2 under pressure is realized in a flow cell of thickness $d = 1.05$ mm and diameter $43d$, heated from below with a ohmic film heater, cooled from above with a water bath. The thermoconvection flows, e.g., the roll pattern of figure 1.9b, are visualized with the *shadowgraph*

[8]The problem 1.2 proposes a first study, at infinite Prandtl number, of relevant nonlinear effects.

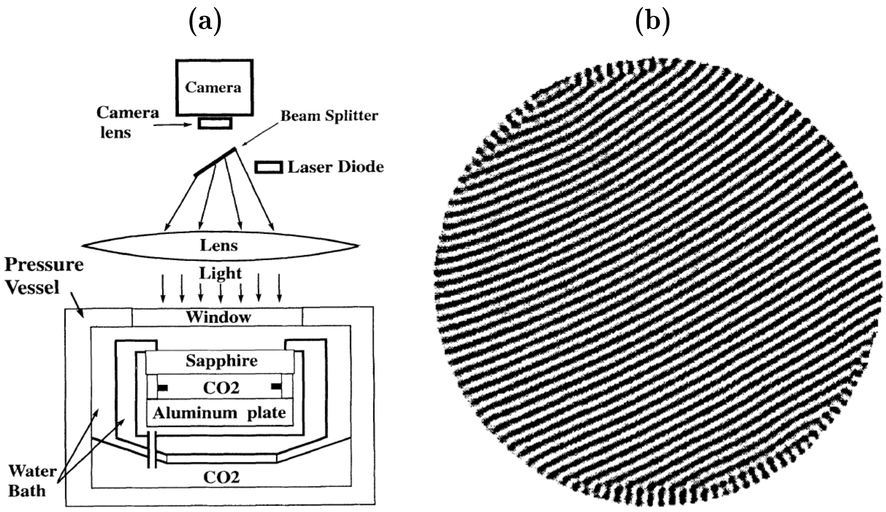

Fig. 1.9 : **(a)** Section of the ***Rayleigh-Bénard Thermoconvection setup*** of Hu *et al.* (1993). **(b)** Top view of a roll pattern obtained near onset, for $R = 1.04 R_c$.

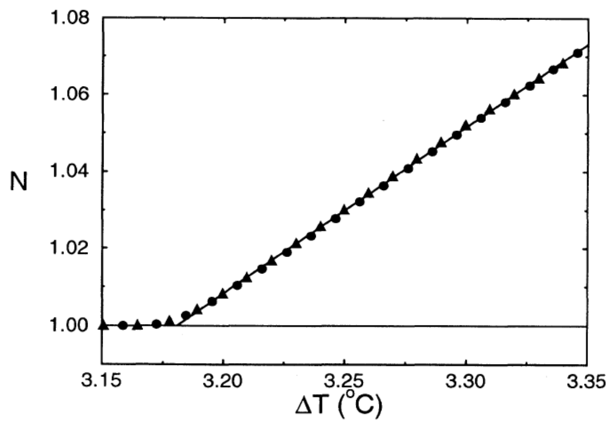

Fig. 1.10 : Nusselt number measured by Hu *et al.* (1993) in their ***RBT experiment***, vs. the applied temperature difference. The triangles are for increasing δT, the circles, for decreasing δT.

method: the refractive index of the fluid depends on T, thus the light rays that pass through the flow cell are more or less deflected depending on T, and an image of an 'average temperature field' is obtained. The knowledge of the power injected in the film heater allows the determination of the heat flux Φ_{heat} that passes through the convection cell. Hence, the Nusselt number Nu, defined in equation (1.74), can be measured. Typical results are shown in figure 1.10. This agrees with the weakly nonlinear formula (1.97). The figure 1.10 thus shows clearly a ***supercritical bifurcation***, without any hysteresis.

Especially at small Prandtl numbers, nonlinear rolls become quickly unstable when the Rayleigh number increases, as shown for instance in Plapp (1997); Bodenschatz *et al.* (2000). These ***secondary instabilities*** have been studied in great details by Busse and coworkers (Busse 2003). After ***tertiary instabilities***, etc... this leads at high Rayleigh numbers to ***turbulent flows***. Relevant informations on turbulent RBT can be found in the review Ahlers *et al.* (2009)... These scenarios of a ***progressive transition to turbulence through a cascade of instabilities*** may be coined as ***'globally supercritical'***.

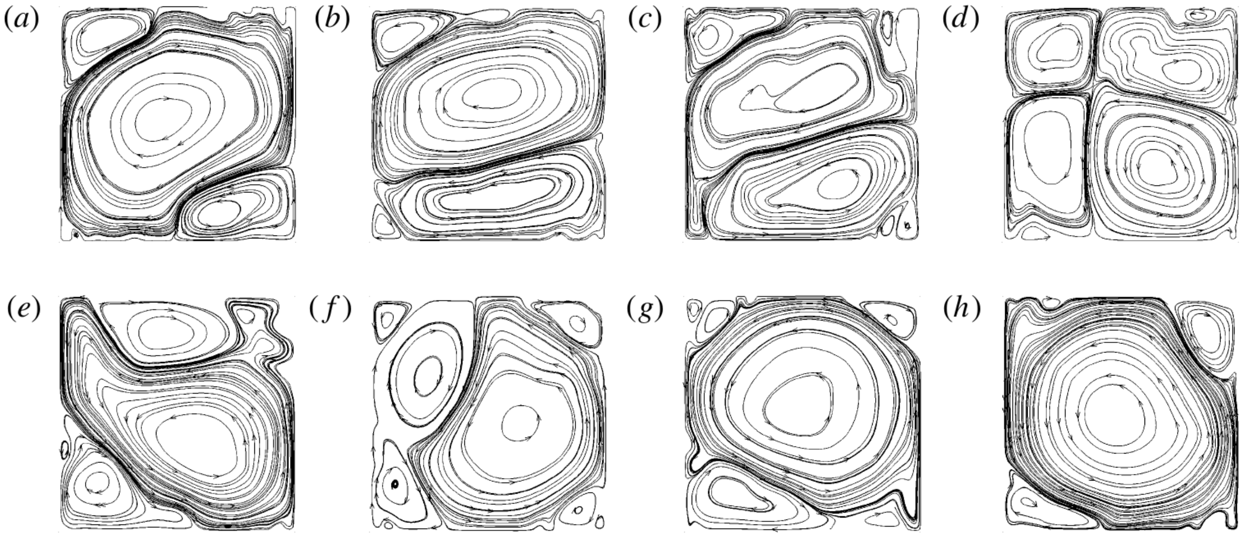

Fig. 1.11 : ***Flow reversal in a 2D RBT cell*** at $R = 5\ 10^7$ and $P = 4.3$, in the numerical study of Podvin & Sergent (2015). Successive snapshots of the streamlines, with arrows that indicate the flow direction, are shown at times $t = 3428$ to 3476 from **a** to **h**. The time unit is $h^2/(\kappa R^{1/2})$.

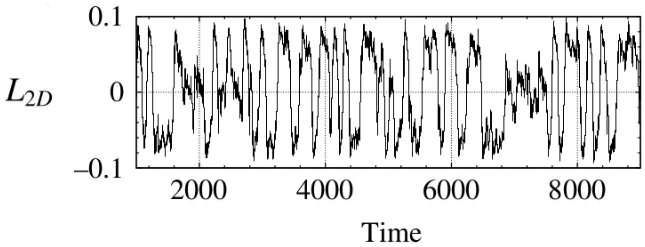

Fig. 1.12 : Global angular momentum of the flow in a ***2D RBT cell*** at $R = 5\ 10^7$ and $P = 4.3$, in the numerical study of Podvin & Sergent (2015). The alternance between positive and negative values reveals ***flow reversals***, as also displayed in figure 1.11.

We terminate this chapter by coming back to ***RBT in confined geometry***. Experiments in small boxes have confirmed the existence of ***chaos*** in fluid systems at the beginning of the 1980s, as explained in Bergé *et al.* (1984). More recently, experiments in quasi-2D cells, of a square cross-section in its largest dimensions, have revealed ***flow reversals***. A numerical experiment that displays such a reversal is shown in figure 1.11. Such reversals do occur in a chaotic manner, as displayed in figure 1.12. As it will explained during the oral lecture, from a phenomenological point of view, there exists an analogy between these flow reversals and the reversals of the Earth's magnetic field, which is created by the thermoconvection flows of the Earth's inner core...

1.8 Exercise and problems

The 'linear' exercise 1.11 is rather elementary, and may be taken soon in the course of the module, once the exercises 1.1 and 1.2 are solved. The exercise 1.11 is followed by some comments, to open on the important topics of ***thermoconvection in the atmosphere***.
The 'nonlinear' problem 1.1 requires that the sessions devoted to chapter 1 are done, whereas the problem 1.2 uses a spectral method of the type introduced in the problem 2.1.

Exercise 1.11 ***Stability analysis of a fluid layer with different thermal stratifications***

We consider a ***layer of a newtonian fluid*** extended in the horizontal xy directions, sandwiched between two horizontal, isothermal plates, placed at $z = \pm d/2$, as sketched on the figure 1.1. We use the notations of the lectures, but study a more general situation with ***two possible different thermal stratifications***. These are defined by the fact that, in the conduction state, the temperature field T_s corresponds

- either to a ***'positive heat flux'*** (PHF)

$$-\lambda_h \frac{dT_s}{dz} > 0 \quad \text{because} \quad T_2 > T_1 \ , \tag{1.98}$$

- or to a ***'negative heat flux'*** (NHF)

$$-\lambda_h \frac{dT_s}{dz} < 0 \quad \text{because} \quad T_2 < T_1 \ . \tag{1.99}$$

In these equations, λ_h denotes the heat conductivity of the fluid.

1 Prove that one has, in the conduction state,

$$T_s = T_0 - \varepsilon\, \delta T \frac{z}{d} \quad \text{with} \quad T_0 = \frac{T_1 + T_2}{2} \ ,$$
$$\delta T = |T_2 - T_1| \ , \quad \varepsilon = +1 \text{ (resp. } -1) \text{ in the PHF (resp. NHF) case.} \tag{1.100}$$

2 Consider a 2D xz perturbation of the conduction state defined by velocity and temperature fields of the form

$$\mathbf{v} = \mathbf{v}(x,z,t) \quad \text{and} \quad T = T_s(z) + \theta(x,z,t) \ . \tag{1.101}$$

Explicit the ***Oberbeck - Boussinesq equations*** that govern the evolution of $\mathbf{v}$, θ and a modified pressure p that intervenes only through its gradient.

3 Establish the dimensionless form of these equations, using the units defined in (1.8), taking care that now $\delta T = |T_2 - T_1|$. The unit of modified pressure is not precised, since the corresponding gradient term will be eliminated in question 4. Denote with a $\tilde{}$ the dimensionless quantities, and drop the $\tilde{}$ at the end. Identify a Rayleigh number and the Prandtl number. Comment, linking to the lectures and explaining the main physical difference between the PHF and NHF cases, with two drawings in the physical space that show the coupling effect in play.

4 By an analogy with the lectures, give the dimensionless form of the linearized vorticity and heat equations that govern the fate of small perturbations of the conduction state, the perturbation fields being the streamfunction ψ and the temperature perturbation θ.

5 We admit that x-homogeneous modes are always damped. We consider normal modes of wavenumber $k \neq 0$ in the x-direction, of the form

$$(\psi,\ \theta) \ = \ (\Psi,\ 1)\ \exp(ikx)\ \sin[n\pi(z+1/2)]\ , \tag{1.102}$$

with Ψ a complex number, $n \in \mathbb{N}^*$. Justify briefly that these modes fulfill the slip and isothermal boundary conditions at the wall. Calculate the characteristic equation that determines the temporal eigenvalue σ associated to these modes. By a study of the two roots $\sigma_\pm$ of this equation, discuss the ***stability properties of the fluid layer depending on its thermal stratification***, i.e., in the
5.1 ***PHF case***
and
5.2 ***NHF case***.

6 We admit that one may extrapolate qualitatively these results to the case of the ***atmospheric boundary layer***, between the soil (over a flat terrain) and a region of uniform flow at 'high' altitude, replacing the static temperature field T_s by the temperature field T_m averaged over the horizontal coordinates in a 'large area'. One may then define

- ***'positive heat flux' atmospheric boundary layers*** where

$$-\lambda_h \frac{dT_m}{dz} \ > \ 0\ , \tag{1.103}$$

- or ***'negative heat flux' atmospheric boundary layers*** where[9]

$$-\lambda_h \frac{dT_m}{dz} \ < \ 0\ , \tag{1.104}$$

with λ_h the heat conductivity of the dry air that constitutes the layer.
In which case does one expect the highest turbulence level ?

Comments on the exercise 1.11 ***Thermoconvection in the atmospheric boundary layer***
The question 6 suggests a classification of ***atmospheric boundary layers*** (ABL) that is meaningful, though another temperature field more relevant to meteorology has to be used: the 'potential temperature' field, but let us say that it is another story... In ***wind energy*** for instance it is well known that the thermal stratification of the ABL and the level of turbulence implied have a strong impact on the wake losses. In a more turbulent ABL, the wake recovery is faster, hence, the wake losses are lower, i.e. a second wind turbine placed downstream in the wake of a first wind turbine gets more wind and produces more power. This is illustrated on the figure 1.13, that shows mean-flows around an operating wind turbine, taken from Abkar & Porté-Agel (2015). They simulate numerically the same wind turbine in 3 different ABL, from top to bottom a 'Convective ABL' (i.e. a PHF ABL with the notations of the exercise), a 'Neutral ABL' (i.e. an ABL with no heat flux) and a 'Stable ABL' (i.e. a NHF ABL). In all cases, the incoming wind has the same wind speed at hub height, $U \simeq 8$ m/s, but the different turbulent intensities (and mean-flow profiles) imply quite different wakes...
Similarly, for the ***dispersion of pollutants***, it is much better to be in a Convective ABL than in a Stable ABL !..

[9] One speaks of an ***'inversion'*** of temperatures, since $dT_m/dz > 0$ occurs more rarely than $dT_m/dz < 0$.

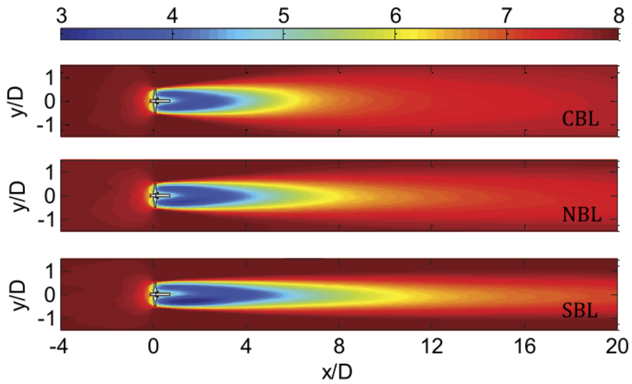

Fig. 1.13 : (color online) From the numerical simulations of Abkar & Porté-Agel (2015): contours of the time-averaged streamwise velocity U [m/s] in the horizontal plane at the level of the hub of a ***wind turbine*** for ***different thermal stratifications*** of the ***atmospheric boundary layer***. Observe the longer (resp. shorter) ***wake*** in the Stable (resp. Convective) Boundary Layer at the bottom (resp. top).

Problem 1.1 ***Lorenz model of slip Rayleigh-Bénard Thermoconvection***

Following Lorenz, we explore a model of slip RBT where the streamfunction

$$\psi \;=\; a(t)\;\sin(kx)\;\cos(\pi z)\;, \tag{1.105}$$

and the temperature perturbation

$$\theta \;=\; b(t)\;\cos(kx)\;\cos(\pi z)\;+\;c(t)\;\sin(2\pi z)\;, \tag{1.106}$$

with $k > 0$ a real number.

0 Specify the physical name and physical meaning of k.

1 Check that these fields satisfy the boundary conditions of slip RBT.

2 Write a Mathematica code to explicit, in the case of a state vector $V = (\psi,\ \theta)$ with ψ given by (1.105) and θ given by (1.106), the equations of slip RBT

$$D\cdot\partial_t V \;=\; L_R\cdot V \;+\; N_2(V,V)\;, \tag{1.107}$$

with $R > 0$ the Rayleigh number. Write the solution on your copy, under the form

$$\begin{aligned}
[D\cdot\partial_t V]_\psi &= \ldots\\
[L_R\cdot V]_\psi &= \ldots\\
[N_2(V,V)]_\psi &= \ldots\\
[D\cdot\partial_t V]_\theta &= \ldots\\
[L_R\cdot V]_\theta &= \ldots\\
[N_2(V,V)]_\theta &= \ldots
\end{aligned}$$

where the r.h.s. are polynomials of $\dot a,\ \dot b,\ \dot c,\ a,\ b,\ c$ (hereafter we do not recall the time dependence, and the superdots denote the time derivative), with coefficients simplified as much as possible. Also, you will use the command `TrigReduce` to expand the z-dependent factor of the coefficient of $a\ c$ in $[N_2(V,V)]_\theta$.

3.a Show that the vorticity equation reduces to an ordinary differential equation (ODE) of order 1 coupling the amplitudes a and b, that you will explicit.

3.b By identifying the coefficients of $\cos(kx)\ \cos(\pi z)$ and $\sin(2\pi z)$ in the heat equation, obtain two ODE of order 1 coupling the amplitudes a, b and c.

3.c If we retain, as Lorenz did it, only these three ODE, are the equations of slip RBT exactly fulfilled ? Conclude on the nature of the Lorenz model.

4 To further reduce the form of the model, implement the changes of variables

$$t' = D_1\, t\ , \quad a = \frac{\sqrt{2}D_1}{k\pi}\, X\ , \quad b = \frac{\sqrt{2}D_1^3}{k^2\pi R}\, Y\ , \quad c = \frac{D_1^3}{k^2\pi R}\, Z \quad \text{with} \quad D_1 = k^2+\pi^2\ . \tag{1.108}$$

Show that the three ODE reduce to the ***'Lorenz system'***

$$\begin{cases} P^{-1}\dot{X} &= \quad Y - X \\ \quad\ \dot{Y} &= rX - Y \ - \ XZ \\ \quad\ \dot{Z} &= \ -bZ \ + \ XY \end{cases} \tag{1.109}$$

with now $\dot{X} = dX/dt'$, $\dot{Y} = dY/dt'$, $\dot{Z} = dZ/dt'$, P the Prandtl number, r and b parameters that depend on R and k. Specify physical names and the physical meaning of r.

5 Explain the physical meaning of the null fixed point $X = Y = Z = 0$ of the Lorenz system.

6 Show by a systematic calculation that other ***fixed points*** appear as soon as r exceeds a value that you will determine. Represent those in the planes (r, X) and (r, Y). What physical phenomenon is revealed by these calculations ?

7 By an 'optimization' calculation based on this study of the Lorenz system, determine the critical value R_c of the Rayleigh number R for which thermoconvection sets in first, and the corresponding critical value k_c of k.

8 From now on, we consider the case $k = k_c$. Specify in this case the expressions of r and b in terms of the parameter $\epsilon = R/R_c - 1$.

9 For $\epsilon > 0$, specify the expressions of X_0, Y_0, Z_0, the amplitudes corresponding to the fixed point of question 6 with X_0 and $Y_0 > 0$, in terms of b and ϵ.
Hereafter, avoid as much as possible to replace b by its actual value, to shorten the expressions.

10.a In order to study the ***secondary stability*** of this fixed point, calculate, in terms of P, b and ϵ, the matrix $[M]$ of the linearized evolution operator that governs the dynamics of small perturbations of $(X_0,\ Y_0,\ Z_0)$. I.e., if we denote the Lorenz system

$$\dot{X} = F_1(X,Y,Z)\ , \quad \dot{Y} = F_2(X,Y,Z)\ , \quad \dot{Z} = F_3(X,Y,Z)\ ,$$

$$[M] = \begin{bmatrix} \partial_X F_1 & \partial_Y F_1 & \partial_Z F_1 \\ \partial_X F_2 & \partial_Y F_2 & \partial_Z F_2 \\ \partial_X F_3 & \partial_Y F_3 & \partial_Z F_3 \end{bmatrix}_{X_0,\ Y_0,\ Z_0} .$$

10.b Calculate the characteristic polynomial $\chi(\sigma) = \det(\sigma[I] - [M])$ where $[I]$ is the identity matrix.

10.c We admit that the eigenvalues of $[M]$, the so-called ***'temporal eigenvalues'***, are of the form

$$\{\sigma_1,\ \sigma_2,\ \sigma_3\} \ = \ \{q+i\omega,\ q-i\omega,\ -s\} \quad \text{with} \quad q\in\mathbb{R},\ \omega\in\mathbb{R}^{+*},\ s\in\mathbb{R}^{+*}\ .$$

What would signal a change of sign of q, from $q<0$ for small $\epsilon>0$, to $q>0$ for $\epsilon>\epsilon_1$?
Right at the point where this change of sign would occur, establish a relation between $\epsilon=\epsilon_1,\ P$ and b.
Check that, for sufficiently large P, a solution ϵ_1 exists in terms of ϵ.

10.d For $P=11$, give a lower bound of ϵ for the ***onset of chaos*** through small perturbations of the studied fixed point. Translate this bound in terms of r and R.

Problem 1.2 ***Weakly nonlinear Rayleigh-Bénard Thermoconvection at infinite Prandtl number with no-slip boundary conditions***

We consider ***Rayleigh-Bénard Thermoconvection*** in a 2D xz extended geometry, in a very viscous fluid of ***infinite Prandtl number***, with ***no-slip boundary conditions***.

First part: linear stability analysis, without symmetry assumptions

1 Specify the ordinary differential equations and the boundary conditions of the ***linear eigenproblem*** that determines the ***temporal eigenvalues*** σ for ***normal modes***

$$\psi \ = \ \Psi(z)\ \exp(ikx)\ ,\quad \theta \ = \ \Theta(z)\ \exp(ikx) \tag{1.110}$$

with a wavenumber $k\neq 0$. You should introduce a notation for the Laplacian.

2 To solve this problem with a ***spectral method***, without any symmetry assumption, justify briefly that it is reasonable to search approximate solutions of the form

$$\Psi(z) \ = \ \sum_{n=1}^{N_z}\Psi_n F_n(z) \quad \text{with} \quad F_n(z) \ = \ (z-1/2)^2\ (z+1/2)^2\ T_{n-1}(2z)\ , \tag{1.111a}$$

$$\Theta(z) \ = \ \sum_{n=1}^{N_z}\Theta_n G_n(z) \quad \text{with} \quad G_n(z) \ = \ (z-1/2)\ (z+1/2)\ T_{n-1}(2z)\ , \tag{1.111b}$$

T_n the n^{th} Chebyshev polynomial of the first kind, N_z the number of z-modes. Specify also the symmetry properties of the functions F_n and $G_n(z)$ under $z\mapsto -z$, knowing that $T_{n-1}(z)$ is even (resp. odd) under $z\mapsto -z$ if n is odd (resp. even).

3 With a geometrical construction that uses a circle of radius 1/2, represent the points

$$z_m \ = \ \tfrac{1}{2}\cos[m\pi/(N_z+1)] \quad \text{for} \quad m\in\ \{1,2,\cdots,N_z\}\ , \tag{1.112}$$

in the case $N_z=8$, and justify briefly that they may be good ***collocation points*** to discretize the equations of the problem.

4.1 We introduce the vectors of the spectral coefficients

$$V_\psi \ = \ \begin{bmatrix}\Psi_1\\ .\\ .\\ .\\ \Psi_{N_z}\end{bmatrix} \quad \text{and} \quad V_\theta \ = \ \begin{bmatrix}\Theta_1\\ .\\ .\\ .\\ \Theta_{N_z}\end{bmatrix}\ . \tag{1.113}$$

By inserting the spectral expansions (1.111a) and (1.111b) into the equations written in question 1, and evaluating the corresponding equations at the collocation points (1.112), show that the discrete approximation of the linear eigenproblem obtained reads

$$0 \;=\; -\,L_1\cdot V_\psi \;-\; ikR\,D_1\cdot V_\theta\;, \tag{1.114a}$$

$$\sigma D_1\cdot V_\theta \;=\; L_2\cdot V_\theta \;+\; ik\,D_2\cdot V_\psi\;, \tag{1.114b}$$

and explicit the formulas that should be used to compute the matrix elements at line m and column n of the square matrices D_1 , D_2 , L_1 and L_2 .

4.2 By eliminating V_ψ as a linear function of V_θ with equation (1.114a), show that one can obtain a generalized eigenvalue problem

$$\sigma D_1\cdot V_\theta \;=\; L\cdot V_\theta \tag{1.115}$$

with L a square matrix that you will define as a function of k, R and the other matrices.

5.0 Write a Mathematica program to solve the linear eigenproblem; it should have this kind of structure:

```
(* Number of modes *) Nz= 6
(* Differential operators *) Dz[u_]:= D[u,z]; Del[u_]:= -k^2 u + Dz[Dz[u]];
(* Base functions for psi *) F[n_,z_]= ...
(* Base functions for theta *) G[n_,z_]= (z-1/2) (z+1/2) ChebyshevT[n-1,2 z]
(* Collocation points *) z[m_]= Cos[m Pi/(Nz+1)]/2.

(* Matrices *) D1= D2= ML1= ML2= IdentityMatrix[Nz];
Do[
   ML1[[m,n]]= ReplaceAll[ ... , z->z[m]];
   D1[[m,n]]= ...
   ML2[[m,n]]= ...
   D2[[m,n]]= ...
 , {m,1,Nz}, {n,1,Nz}]

(* Matrix operators - explicit the wavenumber dependence *)  L1[k_]= ML1; L2[k_]= ML2
(* Matrix L *) L[k_,R_]:= ... + ... Inverse[L1[k]] . D1

(* Spectrum *) spectrum[k_,R_]:= Eigenvalues[{L[k,R],D1}]
(* Most relevant eigenvalue *) sigma1[k_?NumericQ,R_?NumericQ]:= Last[spectrum[k,R]]

(* Neutral value of the Rayleigh number *)
R0[k_?NumericQ]:= R/.FindRoot[Re[sigma1[k,R]],...]
```

5.1 With the command `FindMinimum`, determine the ***critical values*** R_c of the Rayleigh number and k_c of the wavenumber for the onset of no-slip convection. Check that, when you increase N_z from 6 to 8, the 4 first digits of R_c and k_c are unchanged. Comment briefly the physical meaning of the values found for R_c and k_c .

From now on, always use $N_z = 8$, which is sufficient to converge all the computations. Moreover, we consider modes computed at $R = R_c$ and $k = k_c$. The modes evolve at higher R, but we assume that the changes in the eigenfunctions with R are small and can be neglected.

6 With the command `Eigensystem`, check that the eigenvectors V_θ of the linear eigenproblem are such that $|\Theta_n| < 10^{-10}$ either for n odd or n even; the command `Chop` will help to replace small numbers, of absolute value smaller than 10^{-10}, by 0, to test this property. What is the physical meaning of this property, regarding the function $\Theta(z)$?
In particular, specify with 4 digits the temporal eigenvalue σ_2 of the ***less damped mode***, apart from the critical mode which is neutral. Extract the eigenvector V_θ corresponding to σ_2 , compute its eigenfunction $\Theta(z)$, plot it vs z and comment briefly.

7.1 Coming back to the ***critical mode***, extract its eigenvector V_θ , compute its eigenfunction $\Theta(z)$, and normalize this vector such that

$$\Theta(z=0) \;=\; 1 \;. \tag{1.116}$$

Precise the normalized vector V_θ , with 3 digits for each coefficient. Comment briefly.
Plot $\Theta(z)$ vs z and comment briefly.

7.2 With the formula established in question 4.2, compute the vector V_ψ for this mode. Check that, neglecting small coefficients due to rounding errors (the command `Chop` will help), it is purely imaginary. Precise the vector V_ψ/i, with 3 digits for each coefficient. Comment briefly.
Compute the eigenfunction $\Psi(z)$, specify $\Psi(z=0)$ with 4 digits, plot $\Psi(z)/i = \Psi_i(z)$ vs z. Comment.

7.3 Consider the real critical solution defined by

$$\psi_a \;=\; A\;\Psi(z)\;\exp(ik_cx) \;+\; c.c.\;, \quad \theta_a \;=\; A\;\Theta(z)\;\exp(ik_cx) \;+\; c.c.\;, \tag{1.117}$$

with $A \in \mathbb{R}^{+*}$ a small amplitude, which is now unknown. Establish analytical formulas for ψ_a and θ_a in terms of A, $\Psi_i(z)$, $\Theta(z)$ and trigonometric functions of k_cx where the pure imaginary i does not appear. Comment briefly.
With the help of Mathematica, plot the streamlines (the isolines of ψ_a) on two wavelengths in a rectangle in the xz plane. Comment.

7.4 Establish analytical formulas for the fields

$$v_{xa} \;=\; -\,\partial_z\psi_a \quad \text{and} \quad v_{za} \;=\; \partial_x\psi_a \;, \tag{1.118}$$

where the pure imaginary i does not appear. Comment briefly.

7.5 With the Mathematica command `Put`, save on your disk the values of R_c and k_c in a file `Rckc`, the (normalized) functions $\Psi_i(z)$ and $\Theta(z)$ in files `Psii` and `Theta` .

Second part: study of the dominant nonlinear effects at quadratic order

8.1 In the framework of the ***weakly nonlinear analysis***, for $R = R_c(1+\epsilon)$ with $0 < \epsilon \ll 1$, neglecting harmonic modes, we seek an approximate solution of the full problem of the form

$$\psi \;=\; \psi_a \;+\; h.o.t.\;, \quad \theta \;=\; \theta_a \;+\; \theta_\perp \;+\; h.o.t.\;, \tag{1.119}$$

with ψ_a and θ_a given by (1.117), $A \ll 1$. Moreover, the higher order terms ('*h.o.t.*') are of order A^3, whereas

$$\theta_\perp \;=\; A^2\;\Theta_2(z) \tag{1.120}$$

with $\Theta_2(z)$ the solution of an equation of the form

$$0 \;=\; \Theta_2''(z) \;+\; S(z)\;. \tag{1.121}$$

By citing in particular some of the assumptions of the weakly nonlinear analysis, explain the physical origin of this equation, and explicit the analytical form of the source terms $S(z)$.

Indication: $S(z)$ depends on k_c , $\Psi(z)$ and $\Theta(z)$.

8.2 To solve equation (1.121) with the spectral method, we write, similarly to equation (1.111*b*),

$$\Theta_2(z) \;=\; \sum_{n=1}^{N_z} b_n G_n(z)\;, \tag{1.122}$$

and introduce the vector of coefficients

$$V_2 \;=\; \begin{bmatrix} b_1 \\ . \\ . \\ . \\ b_{N_z} \end{bmatrix}\;. \tag{1.123}$$

Show, with the use of the collocation points (1.112), that the discrete approximation of equation (1.121) reads

$$L_2 \cdot V_2 \;=\; S_0 \tag{1.124}$$

with L_2 computed for $k = 0$ and S_0 a vector of coefficients determined by a simple formula.

9.0 Write a Mathematica program that contains a first part similar to the one of question 5.0, to compute the matrix L_2 for $k = 0$, that reads (with the command `Get`) the files `Rckc.m`, `Psii.m` and `Theta.m` to define R_c , k_c , $\Psi_i(z)$ and $\Theta(z)$, that calculates the function $S(z)$, that construct the vector S_0 with the command `Table`, and then solves the linear problem (1.124) with the command `LinearSolve`. Check with the command `Chop` that $b_n \simeq 0$ if n is odd. Reconstruct finally the function $\Theta_2(z)$.

9.1 With Mathematica, plot $\Theta_2(z)$ vs z. Precise in particular the maximal value of $\Theta_2(z)$ with 4 digits. Comment.

Chapter 2

Transition to turbulence in open shear flows

This chapter corresponds to the sessions 4 to 6.

2.1 Generalities

Open shear flows (OSF) are often encountered in ***aerodynamics***, think for instance to the flow around an ***airfoil***, and also in ***hydrodynamics***, think for instance to ***pipe flow*** or ***channel flow***.

For the sake of simplicity, we focus here on ***incompressible fluids*** and ***2D xz flows***, such as the boundary layer flow over a flat plate (figure 2.1a) or flows in channels (figure 2.1b). It is assumed that in the y direction, the boundaries of the system are far away and have a little influence. Not too close to the leading edge, the boundary layer over a flat plate (figure 2.1a) is quasi invariant under translations in the x direction. To simplify, we will consider hereafter ***parallel open shear flows*** that are strictly invariant under translations in the x direction. In the laminar regime, they correspond to velocity and (modified) pressure fields of the form

$$\boxed{\mathbf{v} \;=\; \mathbf{v}_0 \;=\; U(z)\,\mathbf{e}_x\;, \quad p \;=\; p_{\text{static}} + \rho g Z \;=\; p_0 \;=\; -\,Gx}\;, \tag{2.1}$$

with Z the vertical coordinate, G the pressure gradient necessary to sustain the flow if the fluid is viscous. If the fluid is inviscid, $G = 0$.
We want to analyze the ***stability*** of such basic laminar flows.
For this purpose, we introduce ***perturbations*** of velocity and pressure, i.e., we write

$$\boxed{\mathbf{v} \;=\; \mathbf{v}_0 \;+\; \mathbf{u}\;, \quad p \;=\; p_0 \;+\; \widetilde{p}}\;. \tag{2.2}$$

The ***Navier-Stokes*** or ***Euler*** (if $\nu = 0$) ***equation*** (0.11) then gives

$$\partial_t\mathbf{u} \;+\; U' u_z \mathbf{e}_x \;+\; U\partial_x\mathbf{u} \;+\; (\mathbf{u}\cdot\boldsymbol{\nabla})\mathbf{u} \;=\; -\,(1/\rho)\boldsymbol{\nabla}\widetilde{p} \;+\; \nu\boldsymbol{\Delta}\mathbf{u}\;. \tag{2.3}$$

Since the fluid is incompressible,

$$\mathrm{div}\mathbf{u} \;=\; 0\;. \tag{2.4}$$

We introduce dimensionless equations using a length scale h which is the thickness of the mixing layer, the half-width of the channel, ... For the velocity scale, we use

$$U_0 \;=\; \max_z U(z)\;. \tag{2.5}$$

Finally the unit of time is the advection time, or inertial time, $t_0 = h/U_0$.
The dimensionless form of the Navier-Stokes or Euler equation (2.3) is then

$$\partial_t \mathbf{u} \;+\; U' u_z \mathbf{e}_x \;+\; U \partial_x \mathbf{u} \;+\; (\mathbf{u}\cdot\boldsymbol{\nabla})\mathbf{u} \;=\; -\boldsymbol{\nabla}\widetilde{p} \;+\; R^{-1}\boldsymbol{\Delta}\mathbf{u}\;, \tag{2.6}$$

with[1]

$$\text{the } \textit{\textbf{Reynolds number}} \quad \boxed{R \;=\; U_0 h/\nu}\;, \quad R \;=\; \infty \text{ in an inviscid fluid.} \tag{2.7}$$

Contrarily to the problem of the Rayleigh-Bénard thermoconvection which has been studied in the chapter 1, the basic flow creates an anisotropy in the xy plane. Despite this, on the basis of experimental, numerical and theoretical results (the exercise 2.7 is quite relevant at this stage) that we do not detail for the sake of brevity, we assume that it is relevant to focus, firstly, on perturbations that are ***2D xz***. It is convenient then to use a perturbation ***streamfunction*** ψ such that

$$\boxed{\mathbf{u} \;=\; \mathbf{curl}(\psi\;\mathbf{e}_y) \;=\; (\boldsymbol{\nabla}\psi)\times\mathbf{e}_y \;=\; -(\partial_z\psi)\;\mathbf{e}_x \;+\; (\partial_x\psi)\;\mathbf{e}_z}\;. \tag{2.8}$$

We also eliminate the pressure by solving, instead of (2.6), the ***vorticity equation***, which reduces to its component in the y direction,

$$\partial_t(-\Delta\psi) \;+\; \big[\partial_z\big(\mathbf{u}\cdot\boldsymbol{\nabla}u_x\big) - \partial_x\big(\mathbf{u}\cdot\boldsymbol{\nabla}u_z\big)\big] \;=\; R^{-1}\Delta(-\Delta\psi) \;+\; U\partial_x(\Delta\psi) - U''(\partial_x\psi)\;. \tag{2.9}$$

Since the perturbations in these fluid systems are characterized by only one field, the streamfunction ψ, there is no need to introduce a new notation for the local state vector[2]. This streamfunction fulfills

$$\boxed{D\cdot\partial_t\psi \;=\; L_R\cdot\psi \;+\; N_2(\psi,\psi)} \tag{2.10}$$

$$\text{with}\quad D\cdot\partial_t\psi \;=\; -\Delta\partial_t\psi\;,\quad L_R\cdot\psi \;=\; R^{-1}\Delta(-\Delta\psi) \;+\; U\partial_x(\Delta\psi) - U''(\partial_x\psi), \tag{2.11a}$$

$$N_2(\psi,\psi) \;=\; \partial_x\big(\mathbf{u}\cdot\boldsymbol{\nabla}u_z\big) - \partial_z\big(\mathbf{u}\cdot\boldsymbol{\nabla}u_x\big)\;. \tag{2.11b}$$

The boundary conditions, at the 'plates' located at $z = z_\pm$, are,

$$\text{for a viscous fluid, no-slip,} \quad \mathbf{u} \;=\; \mathbf{0} \quad\Longleftrightarrow\quad \partial_x\psi \;=\; \partial_z\psi \;=\; 0\;, \tag{2.12}$$

$$\text{for an inviscid fluid, slip,} \quad u_z \;=\; 0 \quad\Longleftrightarrow\quad \partial_x\psi \;=\; 0\;. \tag{2.13}$$

2.2 Linear stability analysis of plane parallel flows

This linear analysis relies on the calculation of normal modes of the form

$$\psi \;=\; \Psi_n(z)\;\exp(ikx+\sigma t) \;=\; \Psi_n(z)\;\exp[ik(x-c_r t)]\;\exp(kc_i t) \tag{2.14}$$

with $k\neq 0$ the ***wavenumber***[3], n another label to mark normal modes, σ the temporal eigenvalue. Most often the bulk velocity of the basic flow $\langle U\rangle_z > 0$, hence we expect normal modes that are ***waves*** traveling 'to the right' (in the x direction). For this reason we write

$$\sigma \;=\; -i\omega \;=\; -ikc \tag{2.15}$$

[1]Do not mingle the main control parameter R of this chapter, the Reynolds number, with the main control parameter R of chapter 1, the Rayleigh number.

[2]I.e., the local state vector $V = (\psi)$.

[3]One can easily show that x-homogeneous modes are all damped. Therefore, here $k\in\mathbb{R}^*$... Complex values of k may also be relevant, see Section 2.4.

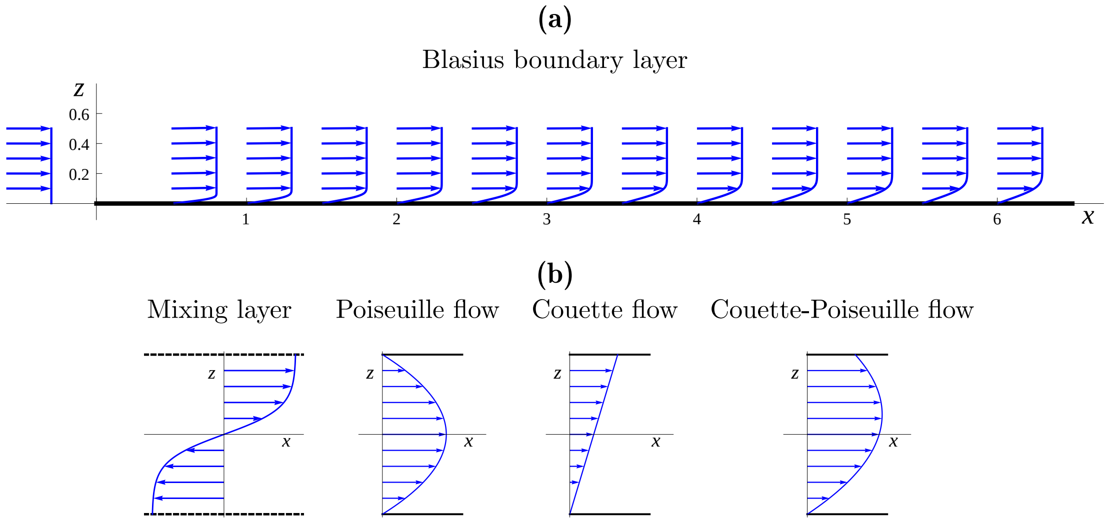

Fig. 2.1 : Examples of laminar 2D ***open shear flows***. **(a)** A slightly non-parallel flow. **(b)** Parallel flows. Our aim in this chapter is to analyze the stability of these flows.

with ω the complex ***angular frequency***, c the complex ***phase velocity***, $c_r > 0$ (most often) the real phase velocity, $kc_i > 0$ (resp. < 0) the growth rate (resp. damping rate). By inserting the form (2.14) in (2.10) and linearizing, we obtain

$$\boxed{(U-c)\Delta\psi \;-\; U''\psi \;=\; (ikR)^{-1}\Delta\Delta\psi} \tag{2.16}$$

which is the ***Orr - Sommerfeld equation*** in a viscous fluid, ***Rayleigh equation*** in an inviscid fluid ($R=\infty$).

The boundary conditions at $z = z_\pm$, are,

$$\text{for a viscous fluid} \quad , \quad \psi \;=\; \partial_z\psi \;=\; 0 \;, \tag{2.17}$$

$$\text{for an inviscid fluid} \quad , \quad \psi \;=\; 0 \;. \tag{2.18}$$

2.2.1 Linear stability analysis of inviscid plane parallel flows

Exercise 2.1 ***Rayleigh's inflection point criterion***

Let us assume that an inviscid plane parallel flow is unstable: there exists (at least) one normal mode (2.14), more simply

$$\psi \;=\; \Psi(z)\;\; \exp[ik(x-c_r t)]\;\; \exp(kc_i t) \;, \tag{2.19}$$

which corresponds to $c_i > 0$.

1 With the Rayleigh equation, calculate $\Psi''(z)$ as a function of $\Psi(z)$, $U(z)$, $U''(z)$, k and c.

2 By multiplication with a suitable function and integration over $z \in [z_-, z_+]$, show that

$$\int_{z_-}^{z_+} \left(k^2|\Psi(z)|^2 + |\Psi'(z)|^2\right)dz \;+\; \int_{z_-}^{z_+} \frac{U''(z)\;|\Psi(z)|^2}{U(z)-c}dz \;=\; 0$$

and, then,

$$\int_{z_-}^{z_+} \frac{U''(z)\;|\Psi(z)|^2}{|U(z)-c|^2}dz \;=\; 0 \;. \tag{2.20}$$

3 Conclude that, if $U'' \neq 0$, U'' must change sign somewhere, i.e. there must exist an ***inflection point*** in the U-profile.

4 Show that, if $U'' = 0$ everywhere, one finds a contradiction, i.e. the base flow is stable.

A typical example of an ***'inflection-point instability'*** is the ***Kelvin-Helmholtz instability*** of the ***mixing layer***, which has been already approached in Plaut (2020), see also the animations on http://emmanuelplaut.perso.univ-lorraine.fr/mf/KH-e.htm.

2.2.2 Linear stability analysis of viscous plane Poiseuille flow

Problem 2.1 ***Linear stability analysis of plane Poiseuille flow with a spectral method***

We analyze the stability of ***plane Poiseuille flow*** (PPF), $U(z) = 1 - z^2$, of a ***viscous fluid***. For this purpose we solve the ***Orr - Sommerfeld equation*** (2.16), here rewritten with the temporal eigenvalue σ,

$$\boxed{\sigma D \cdot \Psi \;=\; -\sigma \Delta \Psi \;=\; L_R \cdot \Psi \;=\; -R^{-1} \Delta\Delta\Psi \;+\; ik(U\Delta\Psi - U''\Psi)} \tag{2.21}$$

with

$$\Delta \;=\; -k^2 \;+\; \frac{d^2}{dz^2} \tag{2.22}$$

and the boundary conditions (2.17),

$$\Psi \;=\; \Psi' \;=\; 0 \quad \text{if} \quad z = \pm 1 \; . \tag{2.23}$$

For this purpose, we use a ***spectral expansion*** of the eigenfunctions $\Psi(z)$, as a sum of simple polynomial functions that fulfill the boundary conditions:

$$\Psi(z) \;=\; \sum_{n=1}^{N} \Psi_n F_n(z) \quad \text{with} \quad F_n(z) \;=\; (z-1)^2\,(z+1)^2\,T_{2n-2}(z) \;=\; (z^2-1)^2\,T_{2n-2}(z) \; , \tag{2.24}$$

T_n the n^{th} Chebyshev polynomial of the first kind, $N = N_z$ the number of z-modes (`Nz` in your code). We retain only the Chebyshev polynomials of even index because we know that the relevant modes correspond to $\Psi(z)$ even under $z \mapsto -z$, i.e. to modes invariant with respect to the midplane reflection symmetry $z \mapsto -z$. To check this, we may test a more general expansion...

1 Start a Mathematica code by defining the functions F_n (`F[n,z]` in your code) and the ***Gauss-Lobatto collocation points***

$$z_m \;=\; \cos[m\pi/(2N+1)] \quad \text{for} \quad m \in \{1, 2, \cdots, N\} \tag{2.25}$$

(`z[m]` in your code). Plot a few functions F_n and the collocation points for various values of N, and comment.

2 By inserting (2.24) in (2.21), we get

$$\sigma \sum_n \Psi_n D \cdot F_n(z) \;=\; \sum_n \Psi_n L \cdot F_n(z)$$

which we want to be fulfilled at the collocation points (2.25):

$$\forall m \; , \quad \sigma \sum_n \Psi_n D \cdot F_n(z_m) \;=\; \sum_n \Psi_n L \cdot F_n(z_m) \; . \tag{2.26}$$

Introducing the vector of the expansion coefficients (or 'spectral coefficients')

$$V = \begin{bmatrix} \Psi_1 \\ \cdot \\ \cdot \\ \cdot \\ \Psi_N \end{bmatrix} , \tag{2.27}$$

show that (2.26) can be written under a matrix form

$$\sigma MD \cdot V = ML \cdot V \tag{2.28}$$

$$\text{with } [MD]_{mn} = D \cdot F_n(z_m) \quad , \quad [ML]_{mn} = L \cdot F_n(z_m) \quad . \tag{2.29}$$

Note that n is a 'column index', m is a 'line index'.

3.a Define in your code the operators D and L_R acting on a general function Ψ or f of z, according to equation (2.21),

```
Dop[f_]:= ...
Lop[f_]:= ...
```

Create the square matrices MD and ML with the good dimension :

```
MatD = MatL = IdentityMatrix[Nz]
```

then, with a double loop, code the rules (2.29):

```
Do[
   Do[
      MatD[[m,n]] = ... ;
      MatL[[m,n]] = ...
     ,{m,1,Nz}]
  ,{n,1,Nz}]
```

Indication : for the derivatives with respect to z to be correctly computed, do not replace too early z by z_m; do this at the end using the `ReplaceAll` command.

3.b To show clearly the control parameters, define

```
MD[k_] = MatD;  ML[k_,R_] = MatL;
```

4 Define the spectrum of the generalized eigenvalue problem (2.28) as

```
spectrum[k_,R_]:= Eigenvalues[{ML[k,R], MD[k]}]
```

and the eigenvalue of the most relevant mode as

```
sigma1[k_?NumericQ,R_?NumericQ]:= Last[Sort[spectrum[k,R]]]
```

The `?NumericQ` will prevent Mathematica from trying to do formal computations on `sigma1`.
By setting k to a typical value, observe the evolution of the spectrum and of the most relevant eigenvalue as a function of R.
Check that PPF is stable at small R but becomes ***unstable*** at large R.

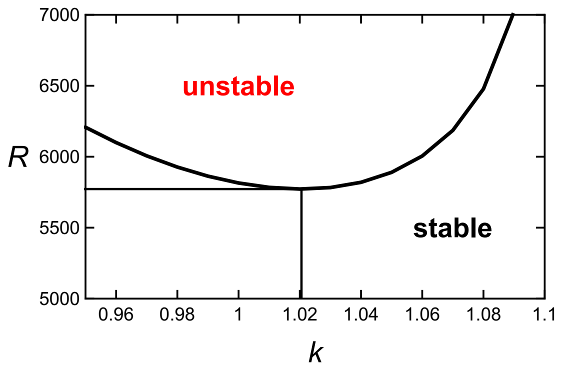

Fig. 2.2 : DIY ! In the wavenumber - Reynolds number plane, ***neutral curve*** for the transition from ***PPF to TS waves***, according to the ***temporal stability analysis*** of problem 2.1. The straight lines show the critical parameters. A zoom out is presented on the figure 2.5.

5 Code the computation of the neutral Reynolds number $R = R_0(k)$ where

$$\mathrm{Re}[\sigma_1(k,R)] \;=\; 0 \tag{2.30}$$

with a command like

```
R0[k_?NumericQ]:= R/.FindRoot[...]
```

to prevent Mathematica from trying to compute formally $R_0(k)$.
Compute a list of values of $R_0(k)$ and plot the corresponding ***neutral curve*** in figure 2.2. Comment.

6.a By minimizing $R_0(k)$ with respect to k, compute the ***critical parameters***

$$k_c \;=\; 1.02\;, \quad R_c \;=\; 5772\;, \quad \omega_c \;=\; 0.269\;, \quad c_c \;=\; 0.264\;. \tag{2.31}$$

Note than ω_c and thus c_c do not vanish: this means that the amplified modes that exist above the neutral curve are ***waves***. Precisely, they are ***TS waves***, in honour of ***Tollmien & Schlichting***, the (german) theoreticians who predicted the existence of these waves in the Blasius boundary layer, during the first part of the 20^{th} century.
Perform ***convergence tests*** by varying the number of modes N_z, for instance, saving your results at given N_z :

```
Put[{Rc,kc,omc},"RckcomcNz"<>ToString[Nz]]
```

then comparing the results obtained with $N_z - 1$ vs N_z modes. For this purpose, load the previous file with the command

```
{Rcold,kcold,omcold} = Get["RckcomcNz"<>ToString[Nz-1]]
```

A reasonable convergence criterion is that k_c, R_c and ω_c do not change by more than 0.1% with $N_z - 1$ vs N_z modes, i.e., concerning k_c, `critkc = (100 Abs[kc/kcold-1]<0.1)` . Determine the minimum number of modes that satisfies this criterion,

$$N_z \;=\; 18\;. \tag{2.32}$$

6.b Explain the physical meaning of the values (2.31) found for k_c and c_c.

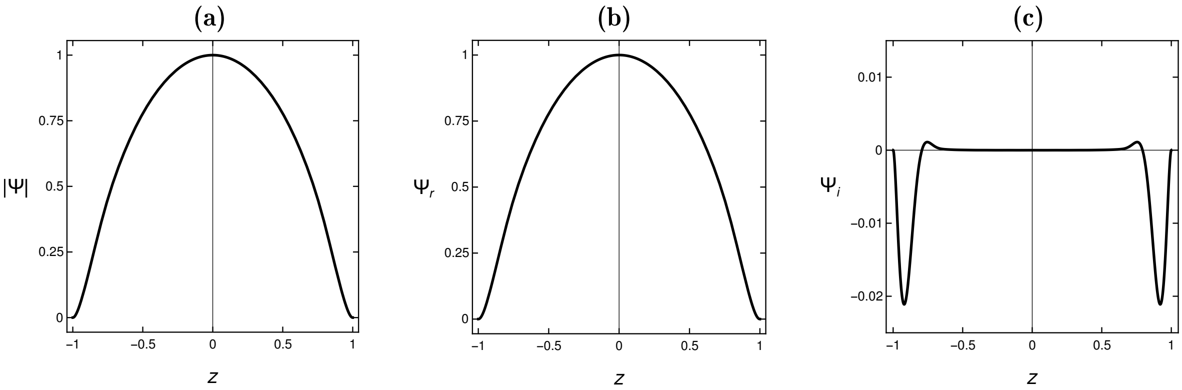

Fig. 2.3 : DIY ! **(a)** Modulus **(b)** real part **(c)** imaginary part of the streamfunction Ψ of the critical ***TS wave***, as a function of the coordinate z.

7.a With the `Eigensystem` command, find the vector V (2.27) that represents the ***critical mode*** eigenfunction $\Psi(z)$. By coding the summation (2.24), compute this function $\Psi(z)$. Normalize it such that

$$\Psi(z=0) \;=\; 1 \;, \tag{2.33}$$

realize the plots asked for in the figure 2.3, and comment.

7.b To prepare weakly nonlinear calculations, save, with the command `Put`, the vector of the spectral coefficients (2.27) of the normalized critical mode eigenfunction $\Psi(z)$ to a file `V1`.

8 Compute a streamfunction that represents PPF with a TS wave

$$\mathbf{v} \;=\; \mathbf{v}_0 \;+\; \mathbf{u} \tag{2.34}$$

with $\mathbf{u}$ deriving from

$$\psi \;=\; A\;\Psi(z)\;\exp(ik_c x) \;+\; c.c. \;=\; 2A\mathrm{Re}[\Psi(z)\;\exp(ik_c x)] \;, \tag{2.35}$$

$A \in \mathbb{R}$ a 'small' amplitude that one cannot compute with such a linear theory, and that you will vary. For this purpose, introduce a streamfunction $\Psi_0(z)$ that represents pure PPF. Take care of the midplane reflection symmetry $z \mapsto -z$: $\Psi_0(z)$ should be odd under $z \mapsto -z$.
Use this to plot the streamlines of PPF with a more or less developped TS wave, $A = 0,\ 0.1$ and 0.2, in figure 2.4.
Comment these plots, in connection with this citation of Reynolds (1895):

'when water is caused by pressure to flow through a uniform smooth pipe,
the motion of the water is ***direct****, i.e., parallel to the sides of the pipe,*
or ***sinuous****, i.e., crossing and re-crossing the pipe,*
according as R is below or above a certain value'.

One might expect that, from the point of view of the linear analysis, nothing interesting happens when R becomes much larger than R_c , i.e., the modes that were amplified at $R \simeq R_c$ become more and more amplified (with a larger and larger growth rate), and also some modes that were damped at $R \simeq R_c$ become amplified. The following exercise shows that this is not so simple !..

(a) $A = 0$:

(b) $A = 0.1$:

(c) $A = 0.2$:

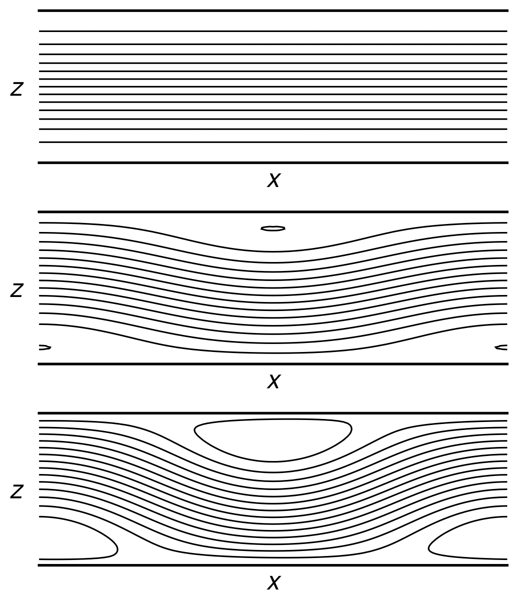

Fig. 2.4 : DIY ! In a vertical slice of the channel, ***streamlines*** of **a:** ***pure PPF***, **b:** ***PPF*** + the ***critical TS wave*** with small amplitude $A = 0.1$, **c:** ***PPF*** + the ***critical TS wave*** with a larger amplitude $A = 0.2$. One wavelength is shown.

Exercise 2.2 ***Linear stability analysis of PPF at high Reynolds number***

1 With the program that you wrote for the problem 2.1, using at least $N_z = 18$ spectral modes, plot the real part of the eigenvalue $\sigma(k, R)$ of the most relevant mode with a streamwise wavenumber

$$k = 0.9$$

versus $R \in [5\ 10^3, 100\ 10^3]$. Observe that this mode is amplified only in a range of Reynolds number $R \in [R_0(k), R_1(k)]$.

2 Code with `FindRoot` the computation of the high Reynolds number $R_1(k)$ at which $\mathrm{Re}[\sigma(k, R)]$ vanishes.

3 Saving the value of $R_1(k)$ to files with names `R1Nz*` and re-reading these files, implement the convergence criterion that $R_1(k)$ does not change by more than 0.01% with $N_z - 1$ vs N_z modes: if $r_{1\mathrm{low}} = R_1(k; N_z - 1)$ and $r_1 = R_1(k; N_z)$, one wants that

$$|r_1/r_{1\mathrm{low}} - 1| \ < \ 10^{-4}\ .$$

Determine according to this criterion the lowest value of N_z that one should use for this study at high Reynolds number, and an estimate of $R_1(k)$ with 2 digits.
Importantly, you should observe that you run into precision problems at high N_z. To increase the precision, define the collocation points with

```
z[m_]= N[Cos[m Pi/(2 Nz+1)],Nz]
```

Hereafter we do no more focus on $k = 0.9$ but explore a range of values of k.

4 With the value of N_z determined in question 3, construct a list `lkR0` of the couples $(k, R_0(k))$ with k the wavenumber, $R_0(k)$ the lower neutral Reynolds number, for discrete k values spanning

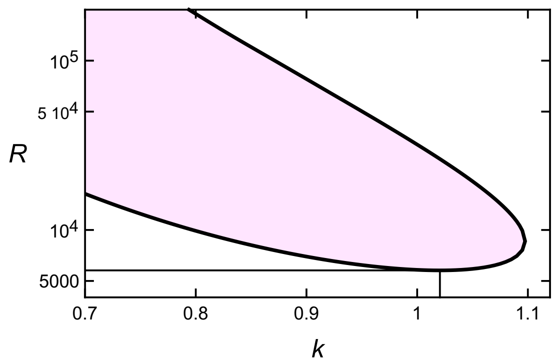

Fig. 2.5 : DIY ! In an extended region of the wavenumber - Reynolds number plane, region of ***linear instability of PPF to TS waves***, according to the ***temporal stability analysis at high Reynolds number***, see exercise 2.2. The straight lines show the critical parameters.

the interval

$$0.7 \ \leq\ k\ \lesssim\ 1.1\ .$$

Construct also a list `lkR1` of the couples $(k, R_1(k))$ with k the wavenumber, $R_1(k)$ the higher neutral Reynolds number, for discrete k values spanning the interval

$$0.8 \ \leq\ k\ \lesssim\ 1.1\ .$$

To compute this second list, use a continuation method: start at large k and decrease k by small steps, using as an estimate of $R_1(k)$ in the `FindRoot` command the value of $R_1(k)$ computed at the previous step.
Join these two lists and plot in figure 2.5, in linear - log scales, the limit of the region where TS waves are amplified in the (k, R) plane, in the intervals

$$0.7 \ \leq\ k\ \leq\ 1.1\ , \quad 5\ 10^3\ \leq\ R\ \leq\ 200\ 10^3\ .$$

5 Explain what happens as $R \to +\infty$ using a theoretical result valid in this limit.

2.3 Weakly nonlinear stability analysis of plane Poiseuille flow

We present here a ***simplified weakly nonlinear analysis*** of ***viscous plane Poiseuille flow*** (PPF), seen as a ‘generic’ example of plane parallel flow. This weakly nonlinear analysis is valid for small values of the ***bifurcation parameter***

$$\boxed{\epsilon \ =\ R/R_c - 1\ \ll\ 1}\ . \tag{2.36}$$

2.3.1 Linear modes basis - Adjoint problem & adjoint modes

The idea is still to use the ***linear modes basis***. We use periodic boundary conditions under $x \mapsto x + 2\pi/k_c$. Therefore, the linear modes are characterized by $\mathbf{q} = (k, n)$ with k the x-wavenumber, integer multiple of k_c, and n an integer which indexes the z-dependence. We denote the ***critical mode***

$$\psi_{1c}\ =\ \Psi(z)\ \exp(ik_c x)\ , \tag{2.37}$$

with $\Psi(z)$ the critical streamfunction. An ***adjoint problem*** and ***adjoint critical mode*** is now defined with the method of section 1.3.

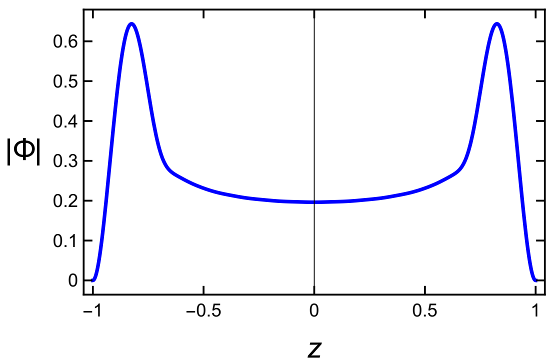

Fig. 2.6 : DIY ! Modulus of the streamfunction of the ***adjoint critical mode*** in PPF, normalized according to the condition (2.43), as a function of the coordinate z.

Exercise 2.3 ***Adjoint problem and adjoint critical mode in PPF***

1 Consider a viscous plane parallel flow (typically, PPF) in a channel with boundaries at $z = \pm 1$ in dimensionless units. Over the streamfunction space, the Hermitian inner product

$$\langle \psi, \ \phi \rangle \ = \ \int_{x=0}^{\lambda_c} \int_{z=-1}^{1} \psi(x,z) \ \phi^*(x,z) \ \frac{dx}{\lambda_c} \ \frac{dz}{2} \ . \qquad (2.38)$$

Focusing on the case of Fourier modes in x, of wavenumber $k = mk_c$ with $m \in \mathbb{Z}^*$,

$$\langle \Psi(z) \ \exp(ikx), \ \Phi(z) \ \exp(ikx) \rangle \ = \ \int_{z=-1}^{1} \Psi(z) \exp(ikx) \ [\Phi(z) \exp(ikx)]^* \ \frac{dz}{2} \ . \qquad (2.39)$$

Show with analytic hand-made calculations that the adjoint operators corresponding to the operators D and L_R (2.11a) characterizing the stability of a plane parallel flow are

$$D \ = \ D^\dagger \ = \ -\Delta \ , \qquad L_R^\dagger \cdot \phi \ = \ -R^{-1} \Delta\Delta\phi \ - \ 2ikU' \partial_z \phi \ - \ ikU\Delta\phi \ . \qquad (2.40)$$

2 With the spectral method of problem 2.1, represent the adjoint critical problem for PPF,

$$\sigma^* D \cdot \phi \ = \ L_R^\dagger \cdot \phi \ , \qquad (2.41)$$

as a matrix problem.

3.a With the command `Get`, read the file `RckcomcNz..` writen during the resolution of problem 2.1, then solve numerically the adjoint problem (2.41) for $k = k_c$, $R = R_c$, and check that there exists an ***adjoint critical mode***

$$\phi_{1c} \ = \ \Phi(z) \ \exp(ik_c x) \qquad (2.42)$$

corresponding to $\sigma = -i\omega_c$.

3.b Calculate the function $\Phi(z)$, plot $|\Phi(z)|$ and comment.

4 Normalize this mode with the condition (1.56),

$$\langle D \cdot \psi_{1c} \ , \ \phi_{1c} \rangle \ = \ \int_{-1}^{1} [D \cdot \Psi \exp(ik_c x)] \ \Phi^* \exp(-ik_c x) \frac{dz}{2} \ = \ 1 \ . \qquad (2.43)$$

For this purpose read the file `V1` written during the resolution of the problem 2.1, to reconstruct the critical mode eigenfunction $\Psi(z)$, and evaluate the scalar product with the not-normalized adjoint mode using `NIntegrate`. Plot the normalized $|\Phi(z)|$ in figure 2.6, and comment. Save the spectral coefficients of the normalized adjoint streamfunction $\Phi(z)$ to a file `U1`.

2.3.2 Simplified form of the weakly nonlinear solution: active and passive modes

We distinguish between ***active*** and ***passive modes***.

- The ***active modes*** correspond to $\mathbf{q} = \mathbf{q}_c = (k_c, 1)$ or $\mathbf{q}_c^* = (-k_c, 1)$ and have eigenvalues

$$\sigma(\mathbf{q}_c, R) \;=\; -i\omega_c \;+\; (1+is)\epsilon/\tau_0 \;+\; O(\epsilon^2)\;, \tag{2.44a}$$
$$\sigma(\mathbf{q}_c^*, R) \;=\; +i\omega_c \;+\; (1-is)\epsilon/\tau_0 \;+\; O(\epsilon^2)\;, \tag{2.44b}$$

  with $\tau_0 > 0$ the characteristic time of the instability, s the linear frequency-shift coefficient.

- The ***passive modes*** correspond to $\mathbf{q} \neq \mathbf{q}_c, \mathbf{q}_c^*$ and are short-living (rapidly damped),

$$\sigma(\mathbf{q}, R) \;=\; \sigma_r(\mathbf{q}, R) \;+\; i\sigma_i(\mathbf{q}, R) \quad \text{with} \quad \sigma_r(\mathbf{q}, R) \;<\; \sigma_1 \;<\; 0\;. \tag{2.45}$$

The weakly nonlinear solution is seeked as

$$\boxed{\psi \;=\; \psi_a \;+\; \psi_\perp} \tag{2.46}$$

with the ***active modes*** leading term

$$\boxed{\psi_a \;=\; A(t)\;\exp(-i\omega_c t)\;\psi_{1c} \;+\; c.c. \;\ll\; 1}\;, \tag{2.47}$$

and $\psi_\perp \;\ll\; \psi_a$ ***passive modes*** terms. It is quite important to insert the oscillating factor $\exp(-i\omega_c t)$. Indeed, if one inserts this ansatz in the linearized problem, one obtains

$$\begin{aligned}\left(\frac{dA}{dt} - i\omega_c A\right)\;\exp(-i\omega_c t)\;D\cdot\psi_{1c} \;+\; c.c. \;&=\; A\;\exp(-i\omega_c t)\;L_R\cdot\psi_{1c} \;+\; c.c.\\ &=\; \sigma(\mathbf{q}_c, R)\;A\;\exp(-i\omega_c t)\;D\cdot\psi_{1c} \;+\; c.c.\end{aligned} \tag{2.48}$$

By projection onto the adjoint critical mode ϕ_{1c} , one gets

$$\frac{dA}{dt} - i\omega_c A \;=\; \sigma(\mathbf{q}_c, R)\;A \quad\Longleftrightarrow\quad \frac{dA}{dt} \;=\; [\sigma(\mathbf{q}_c, R) + i\omega_c]\;A \;\sim\; (1+is)\frac{\epsilon}{\tau_0}\;A \tag{2.49}$$

according to the expansion (2.44). This shows that A is a ***slowly varying*** amplitude, i.e. that the active modes are ***'long-living'***.

At leading order, the ***passive modes*** are created by the nonlinear terms

$$N_2(\psi_a, \psi_a) \;=\; |A(t)|^2\;[N_2(\psi_{1c}, \psi_{1c}^*) \;+\; c.c.] \;+\; [A^2(t)\;\exp(-2i\omega_c t)\;N_2(\psi_{1c}, \psi_{1c}) \;+\; c.c.]\;. \tag{2.50}$$

The analysis is simplified in that we disregard, in a first approach, the harmonic modes in $\exp[\pm 2i(k_c x - \omega_c t)]$, that we 'neglect'. This is a very crude approximation, you might try to avoid it by computing these harmonic modes and their feedback on the critical mode...
Thus, we will assume that $\psi_\perp$ contains only an x-homogeneous contribution,

$$\psi_\perp \;\simeq\; A_0(t)\;\psi_{20}\;. \tag{2.51}$$

By identification of the x-homogeneous, passive part of the equations, one gets

$$\frac{dA_0}{dt}\;D\cdot\psi_{20} \;=\; A_0\;L_R\cdot\psi_{20} \;+\; |A(t)|^2\;[N_2(\psi_{1c}, \psi_{1c}^*) \;+\; c.c.]\;. \tag{2.52}$$

We solve this equation by ***quasistatic elimination***, assuming

$$A_0 \;=\; |A|^2 \;, \quad \text{therefore} \quad \frac{dA_0}{dt} \;\ll\; A_0 \quad \text{and} \quad 0 \;=\; L_R \cdot \psi_{20} \;+\; [N_2(\psi_{1c}, \psi_{1c}^*) \;+\; c.c.] \;. \tag{2.53}$$

Thus

$$\boxed{\psi_\perp \;\simeq\; |A|^2 \;\psi_{20}} \;. \tag{2.54}$$

Note the similarity with the equations (1.70) and (1.73).
However, all the information concerning pressure has been lost when we considered the vorticity equation (2.9) instead of the Navier-Stokes equation (2.6). This is not dangerous as far as modulated modes like the critical mode are concerned: to them corresponds a modulation of pressure, which is not very important. On the contrary, when we want to calculate an x-homogeneous mode like ψ_{20}, we must care with the pressure: modifying the mean pressure gradient for instance would translate in a change of the head losses, which are quite important from an energetical point of view. Therefore, to calculate ψ_{20} with the most natural condition of ***fixed mean pressure gradient - fixed head losses***, we must come back to the Navier-Stokes equation (2.6). The streamfunction ψ_{20} thus corresponds to a correction of the basic flow $U(z)\mathbf{e}_x$, of the form $U_2(z)\mathbf{e}_x$, which is driven by the quasistatic equation

$$R_c^{-1} U_2''(z) \;=\; [(\mathbf{u}_1 \cdot \boldsymbol{\nabla})\mathbf{u}_1^* \;+\; c.c.]_x \tag{2.55}$$

with

$$\mathbf{u}_1 \;=\; -\,\partial_z[\Psi(z)\;\exp(ik_c x)]\;\mathbf{e}_x \;+\; \partial_x[\Psi(z)\;\exp(ik_c x)]\;\mathbf{e}_z \tag{2.56}$$

the velocity field of the critical mode (2.37).

Exercise 2.4 ***General form of the nonlinear source terms for the homogeneous mode***

Separating the critical streamfunction into real and imaginary parts according to

$$\Psi(z) \;=\; \Psi_r(z) \;+\; i\Psi_i(z) \;, \tag{2.57}$$

show with formal computations performed with Mathematica that the nonlinear source term in equation (2.55) can be simplified,

$$[(\mathbf{u}_1 \cdot \boldsymbol{\nabla})\mathbf{u}_1^* \;+\; c.c.]_x \;=\; 2k_c[\Psi_r''(z)\Psi_i(z) - \Psi_r(z)\Psi_i''(z)] \;. \tag{2.58}$$

Exercise 2.5 ***Homogeneous passive mode in PPF with a fixed mean pressure gradient***

The equation (2.55) can be integrated once to obtain

$$R_c^{-1} U_2'(z) \;=\; 2k_c[\Psi_r'(z)\Psi_i(z) - \Psi_r(z)\Psi_i'(z)] \;, \tag{2.59}$$

where the constant of integration vanishes[4]. This equation (2.59) shows that $U_2'(z)$ vanishes if $z = \pm 1$. Therefore, $U_2(z)$ satisfies the same boundary conditions as $\Psi(z)$, i.e.

$$U_2 \;=\; U_2' \;=\; 0 \quad \text{if} \quad z = \pm 1 \;. \tag{2.60}$$

[4]One can show this by integrating the equation (2.59) once more, writing the boundary conditions $U_2(\pm 1) = 0$, and using the fact that $\Psi(z)$ is even under $z \mapsto -z$.

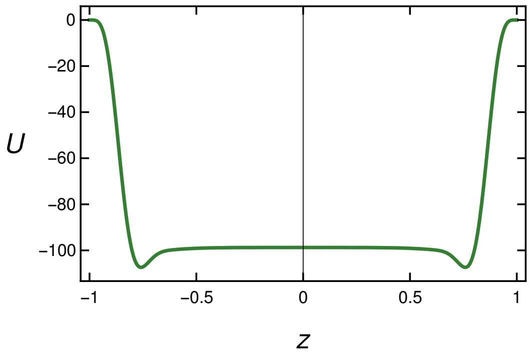

Fig. 2.7 : DIY ! Correction $U_2(z)$ to the mean flow in a channel, due to the presence of the ***critical TS wave***, at order A^2.

Finally, the equation (2.55) can be rewritten

$$-\,D \cdot U_2 \;=\; \Delta U_2(z) \;=\; U_2''(z) \;=\; 2R_c k_c [\Psi_r''(z)\Psi_i(z) - \Psi_r(z)\Psi_i''(z)] \;. \tag{2.61}$$

The operator D already encountered in the linear analysis (see equation 2.21) is implied, and acts on the x-homogeneous field U_2 which satisfies the same boundary conditions (2.60) as the field Ψ of the linear problem (see equation 2.23). Therefore, the spectral code constructed in problem 2.1 can be re-used to solve equation (2.61).

1 In a new notebook, extract a part of the code of problem 2.1 to compute the matrix MD that represents D for $k = 0$, with the spectral method.

2 With the command `Get`, read the files `RckcomcNz..` and `V1` written during the resolution of problem 2.1, to define the critical parameters R_c and k_c, and the critical streamfunction $\Psi(z)$. Separate it into real and imaginary parts, and evaluate the source term, the r.h.s. of equation (2.61), at the collocation points (2.25), to compute a source vector S_0 such that

$$-\,MD \cdot V_0 \;=\; S_0 \;, \tag{2.62}$$

with V_0 the vector of the spectral coefficients of $U_2(z)$.

3 Solve the problem (2.62) with the command `LinearSolve`, to compute V_0, then $U_2(z)$. Plot $U_2(z)$ in figure 2.7 and explain the physics behind.

4 Save the vector of the spectral coefficients of $U_2(z)$ to a file `U2`.

Comments on exercises 2.4 and 2.5 and on the mechanisms in play

One may show that the source terms in the equation (2.55) read, in an alternate manner,

$$[(\mathbf{u}_1 \cdot \boldsymbol{\nabla})\mathbf{u}_1^* \;+\; c.c.]_x \;=\; -\,\rho^{-1}\,\partial_z \tau_{xz}^t \tag{2.63}$$

with the ***main Reynolds stress***

$$\tau_{xz}^t \;=\; -\,\rho\,\langle u_{1x} u_{1z} \rangle_x \;=\; -\,\rho\,\langle u_{1x} u_{1z} \rangle_t \;. \tag{2.64}$$

A geometrical interpretation of τ_{xz}^t is presented in Plaut *et al.* (2008). These authors also advocate and precise the ***'Reynolds-Orr amplification mechanism'***, which may be viewed as the 'motor' of the TS waves. The Reynolds stress (2.64) plays thus an important role in the nonlinear mechanisms linked to the transition to turbulence. An energetic analysis shows that it plays also a role at the linear stage. Note finally that, for the study of fully turbulent flows, ***Reynolds stresses*** that are defined as in (2.64) are also quite important, see e.g. Plaut *et al.* (2021), which is somehow a follow-up of this module !..

2.3.3 Feedback at order A^3

In the nonlinear regime, one has of course to add, in the r.h.s. of the linearized equation (2.48), the terms

$$N_2(\psi,\psi) \;=\; N_2(\psi_a,\psi_a) \;+\; N_2(\psi_a,\psi_\perp) \;+\; N_2(\psi_\perp,\psi_a) \;+\; h.o.t. \tag{2.65}$$

To obtain the amplitude equation for $A(t)$, we have to project these terms onto the adjoint critical mode ϕ_{1c}, and collect the resonant terms N, such that

$$\langle N,\ \phi_{1c}\rangle \;\neq\; 0\ .$$

From the equation (2.47) and (2.54), we know that

$$\psi_a \;=\; A(t)\ \exp(-i\omega_c t)\ \psi_{1c} \;+\; c.c. \quad \text{and} \quad \psi_\perp \;\simeq\; |A(t)|^2\ \psi_{20}\ , \tag{2.66}$$

with $\psi_{1c} \propto \exp(ik_c x)$ and ψ_{20} independent of x. Therefore, at leading order,

$$\langle N_2(\psi,\psi),\ \phi_{1c}\rangle \;=\; g\ |A(t)|^2 A(t) \tag{2.67}$$

with the ***feedback coefficient***

$$g \;=\; \langle N_2(\psi_{1c},\psi_{20}) + N_2(\psi_{20},\psi_{1c}),\ \phi_{1c}\rangle\ . \tag{2.68}$$

This general theoretical expression becomes more concrete if one rewrites the nonlinear term in the vorticity equation (2.10) as

$$\widetilde{N}_2(\mathbf{u}_a,\ \mathbf{u}_b) \;=\; \partial_x\big(\mathbf{u}_a\cdot\boldsymbol{\nabla}u_{zb}\big) - \partial_z\big(\mathbf{u}_a\cdot\boldsymbol{\nabla}u_{xb}\big)\ . \tag{2.69}$$

Then the ***nonlinear resonant term***

$$S_2(x,z) \;=\; \widetilde{N}_2(\mathbf{u}_1,\ U_2\mathbf{e}_x) \;+\; \widetilde{N}_2(U_2\mathbf{e}_x,\ \mathbf{u}_1)\ , \tag{2.70}$$

with $\mathbf{u}_1$ given by equation (2.56), and the feedback coefficient

$$g \;=\; \langle S_2(x,z),\ \phi_{1c}(x,z)\rangle \;=\; \int_{z=-1}^{1} S_2(0,z)\ \Phi^*(z)\ \frac{dz}{2}\ . \tag{2.71}$$

Exercise 2.6 ***Feedback coefficient in PPF with a fixed mean pressure gradient***

For PPF, code the computation of the feedback coefficient (2.71) with Mathematica.

1 In a new Notebook, for two velocity fields $\mathbf{u}_a = u_{xa}\mathbf{e}_x + u_{za}\mathbf{e}_z$ and $\mathbf{u}_b = u_{xb}\mathbf{e}_x + u_{zb}\mathbf{e}_z$, write a function `N2[uxa,uza,uxb,uzb]` that codes $\widetilde{N}_2(\mathbf{u}_a,\ \mathbf{u}_b)$ defined by equation (2.69).

2 Read the file `RckcomcNz..` to define the critical parameters R_c and k_c ; the files `V1`, `U1`, `U2` to reconstruct the functions $\Psi(z)$, $\Phi(z)$ and $U_2(z)$.
Write a function `S2[x,z]` that codes $S_2(x,z)$ defined by equation (2.70).

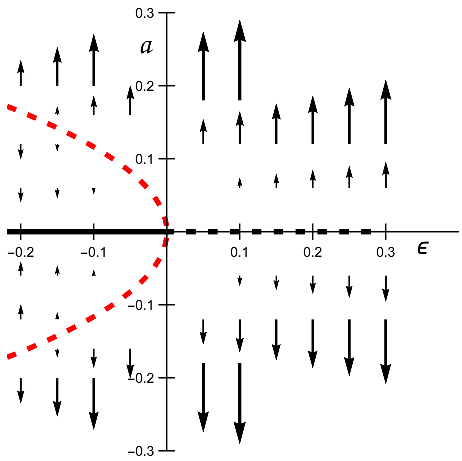

Fig. 2.8 : DIY ! ***Bifurcation diagram*** of the amplitude equation (2.76), with the same convention as in figure 1.6, to which it should be compared. The arrows now show vectors $(0,\ da/dt)$ when $a(t)$ evolves according to equation (2.76), from an initial condition which is not a fixed point.

3 Compute with `NIntegrate` the feedback coefficient g defined by equation (2.71).
Check that, when separated into real and imaginary parts,

$$g \ = \ g_r \ + \ ig_i \quad \text{with} \quad g_r \ \text{ of a definite sign, } g_r \ > \ 0 \ , \tag{2.72}$$

and give a numerical estimate of g_r with 2 digits,

$$g_r \ = \ 39 \ . \tag{2.73}$$

In conclusion, gathering the linear and lowest order nonlinear terms in the evolution equation

$$D \cdot \partial_t \psi \ = \ L_R \cdot \psi \ + \ N_2(\psi, \psi)$$

projected onto ϕ_{1c}, we obtain, according to (2.48) and (2.67), the ***complex amplitude equation***

$$\boxed{\frac{dA}{dt} \ = \ (1+is)\frac{\epsilon}{\tau_0}\ A \ + \ (g_r + ig_i)|A|^2 A} \ . \tag{2.74}$$

It is useful to use a polar representation of the amplitude,

$$A \ = \ |A| \ \exp(i\phi) \ . \tag{2.75}$$

The modulus $a = |A|$ then satisfies the real ***amplitude equation***

$$\boxed{\frac{da}{dt} \ = \ \frac{\epsilon}{\tau_0}\ a \ + \ g_3 a^3} \quad \text{with} \quad g_3 \ = \ g_r \ > \ 0 \ . \tag{2.76}$$

This is the generic amplitude equation of a ***subcritical pitchfork bifurcation***. The ***anti-saturation*** effect traduced by the fact that $g_3 > 0$ has the consequence that nonlinear terms enhance the instability for $\epsilon > 0$. Therefore, no stationary solutions or 'fixed points' exist for $\epsilon > 0$. They exist on the contrary for $\epsilon < 0$, i.e., below ('sub') the onset of the bifurcation, and are given by

$$a \ = \ \pm\sqrt{-\epsilon/(\tau_0 g_3)} \ . \tag{2.77}$$

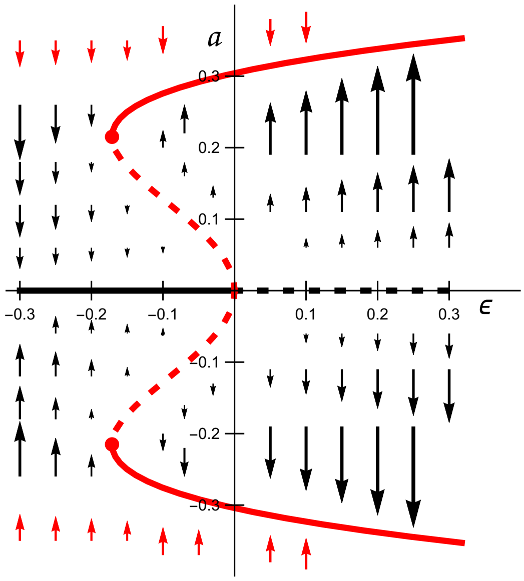

Fig. 2.9 : DIY ! ***Bifurcation diagram*** of the amplitude equation (2.78), with the same convention as in figure 2.8, to which it should be compared. The gray (red online) disks show the turning points where saddle-node bifurcations occur. The black arrows now show vectors $(0, \ da/dt)$ when $a(t)$ evolves according to equation (2.78), from an initial condition which is not a fixed point. Far from the origin, da/dt becomes large, hence the gray (red online) arrows have a length divided by a factor 10, as compared with the black arrows.

However, they are unstable vs perturbations of the amplitude, as shows the corresponding bifurcation diagram figure 2.8. Within this model, for $\epsilon > 0$ the amplitude $a(t)$ goes to infinity, if one starts with an initial condition $a(0) \neq 0$: one faces a very strong instability of the basic flow.

However, to have $|a(t)| \longrightarrow +\infty$ in many cases is not quite physical. A more relevant model can be obtained, phenomenologically, by adding a saturation term at order A^5 or a^5 to the r.h.s. of equation (2.76), thus respecting the symmetry properties of the system. The new ***amplitude equation*** thus obtained,

$$\boxed{\frac{da}{dt} \;=\; \frac{\epsilon}{\tau_0}\;a \;+\; g_3 a^3 \;-\; g_5 a^5} \quad \text{with} \quad g_3, g_5 \;>\; 0 \;, \tag{2.78}$$

corresponds to the bifurcation diagram of figure 2.9. The characteristic time τ_0 can be easily scaled out by a change of the unit of time, i.e., one can assume $\tau_0 = 1$. The bifurcated stationary solutions of (2.78) with $\tau_0 = 1$ are easily parametrized by a as

$$\epsilon \;=\; \epsilon(a) \;=\; -\,g_3 a^2 \;+\; g_5 a^4 \;. \tag{2.79}$$

For small ϵ and a, the two branches of solutions parametrized by this polynomial approach asymptotically the branches of the lower-order amplitude equation (2.76), which are given by equation (2.77) and displayed in figure 2.8. However, at ***'turning points'*** defined by

$$a_{\rm tp} \;=\; \pm\sqrt{g_3/(2g_5)} \quad \text{and} \quad \epsilon_{\rm tp} \;=\; -\,g_3^2/(2g_5) \;, \tag{2.80}$$

the branches turn to the right of the bifurcation diagram of figure 2.9. Exactly as one passes the turning points, the solutions become stable, within the framework of equation (2.78). Since in the

real physical systems there are many degrees of freedom, one typically passes from a 'saddle' fixed point, for $|a| < a_{\rm tp}$, i.e., a solution that has many stable modes and at least one unstable mode, to a 'node' fixed point, for $|a| > a_{\rm tp}$, i.e., a solution that has one more stable mode, and, in some cases, is completely stable. This phenomenon is therefore called a ***'saddle-node bifurcation'***.
A comparison between the figure 1.6 and 2.9 shows that the instability of the basic flow (or state), when $\epsilon > 0$, is 'stronger' than in the supercritical case, since one typically goes, even for quite small values of ϵ, to a finite value of a.
It must also be remarked that, in the interval $\epsilon_{\rm tp} < \epsilon < 0$, there exist three stable solutions of the dynamical system described by the equation (2.78) : the trivial solution $a = 0$ (corresponding to the basic flow) and two bifurcated solutions defined by (2.79). Therefore this model displays ***bistability***. ***Hysteretic*** behaviours can consequently happen: if one starts with a weakly perturbed basic flow, and increases R i.e. ϵ, the transition to TS-waves will occur only at $\epsilon \simeq 0$ i.e. $R \simeq R_c$. If one then decreases R and ϵ, the TS-waves will probably survive down to the turning point where they disappear.

2.4 About spatial and spatio-temporal stability theories

In the ***temporal linear stability theory***, we have considered modes of the linearized problem of the form

$$\exp[i(kx - \omega t)] \quad \text{with} \quad k \in \mathbb{R} \text{ the wavenumber,} \quad \omega = \omega(k) \in \mathbb{C} \text{ the temporal eigenvalue.} \tag{2.81}$$

However, since there exists in general a non-vanishing mean flow, a ***spatial linear stability theory*** is also relevant. Within this approach, one seeks to calculate modes of the linearized problem of the form

$$\exp[i(kx - \omega t)] \quad \text{with} \quad \omega \in \mathbb{R} \text{ the angular frequency,} \quad k = k(\omega) \in \mathbb{C} \text{ the spatial eigenvalue.} \tag{2.82}$$

Using a decomposition of k in real and imaginary parts,

$$k \;=\; k_r + ik_i \;, \tag{2.83}$$

we get

$$\exp[i(kx - \omega t)] \;=\; \exp[i(k_r x - \omega t)]\; \exp(-k_i x) \;. \tag{2.84}$$

Usually, in unstable flows, modes with $k_i < 0$ exist, which are amplified as x increases with the ***spatial rate of amplification*** or ***spatial growth rate*** $-k_i$ ... An example of spatial stability analysis is given in the problem 2.2; see also the corresponding figure 2.14.
In fact, a ***spatio-temporal theory*** may also be developped, where the spatio-temporal response to a perturbation localized in time and space is calculated. The interested reader should for instance immerse himself in Schmid & Henningson (2001).

2.5 Short review of transition in Open Shear Flows - Applications to aerodynamics

Reviews on the nonlinear behaviour of OSF can be found in Huerre & Rossi (1998); Drazin (2002). Numerical computations confirm the subcritical character of the transition to ***Tollmien-Schlichting (TS) waves***. However, typically, these waves are unstable vs three-dimensional

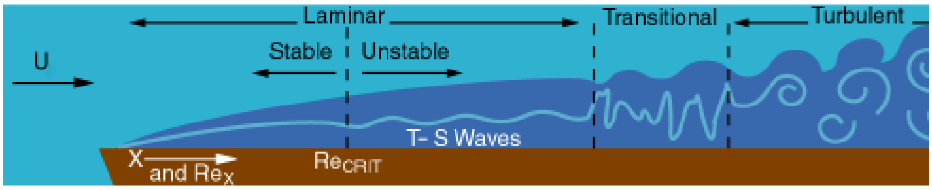

Fig. 2.10 : (color online) Sketch of the ***transition to turbulence in a boundary layer*** placed in a laminar inflow, from the DVD *Multimedia Fluid Mechanics* by Homsy *et al.* 2004 Cambridge University Press.

perturbations. Therefore, a rapid ***transition to turbulence*** often happens in OSF. If the upstream flow (or 'inflow') has a high level of perturbations, ***bypass transition*** can occur, where the flow goes even more rapidly, and 'directly', to turbulence, without the apparition of 2D TS waves.

Also, as already mentioned in section 2.4, the transition to turbulence is generally a ***spatio-temporal problem***. This is obvious in non-parallel flows, like ***boundary layers***, where the local Reynolds number increases with the streamwise coordinate x. There the turbulence sets in at a 'particular' distance from the leading edge, as sketched in the figure 2.10. This 'particular' distance depends on the level and on the nature of the perturbations that are contained in the inflow. This is illustrated in the ***'numerical experiments'*** of Schlatter *et al.* (2010) shown in figure 2.11 and 2.12. In these numerical simulations, which use the 'large-eddy simulation technique', a 2D 'harmonic' forcing is applied close to the inlet of the system, the leftmost segment of figure 2.11*a,b*. This 'harmonic' forcing is a bulk force applied in the wall-normal direction z, localized in the xz plane but independent of the spanwise coordinate y. It is 'harmonic' because it oscillates sinusoidally in time with an angular frequency ω that is close to the critical frequency ω_c of the TS waves. The localization of this harmonic forcing coincides with the green vortex, the leftmost green segment of figure 2.11*a,b*. This harmonic forcing produces ***TS waves*** that first decay with x, but then are amplified due to the natural instability of the Blasius boundary layer, as seen by the green vortices which are regularly spaced in the x-direction, and of a growing intensity in the second right half of the flow region in the figure 2.11*a,b*. The ***three-dimensional instabilities*** of the TS waves and the ensuing ***transition to turbulence*** is clearly visible on the right of these figures. To trigger these three-dimensional instabilities, some 'noise' has been added with a bulk force localized in the same region where the harmonic forcing is acting, this bulk force now depending on the spanwise coordinate y in a random manner. When this force is constant in time, one obtains the scenario of figure 2.11*a*, whereas, when this force depends on time in a random manner, one obtains the scenario of figure 2.11*b*, with an 'earlier' transition to turbulence, in terms of x. A 3D visualization of a case similar to the one of figure 2.11*a* is shown in figure 2.11*c*. One sees first, from left-bottom to right-up, the pattern of TS waves, then a pattern of 3D 'Λ-vortices', then smaller vortices that become more and more turbulent; in addition, low speed blue 'streamwise streaks' are also visible. They indicate a reduction of the average flow velocity. Depending on the global conditions, one also usually observes an ***increase of the drag*** exerted by the fluid on the plate...

If one adds in the inflow, or near the edge of the system, a completely 3D noise that is sufficiently strong, to simulate 'natural free-stream turbulence', even if the harmonic forcing is still present, a quite different scenario is observed, as displayed in the figure 2.12. In this ***bypass transition scenario***, no TS waves appear, but blue and red streamwise 'streaks' come in and break rather

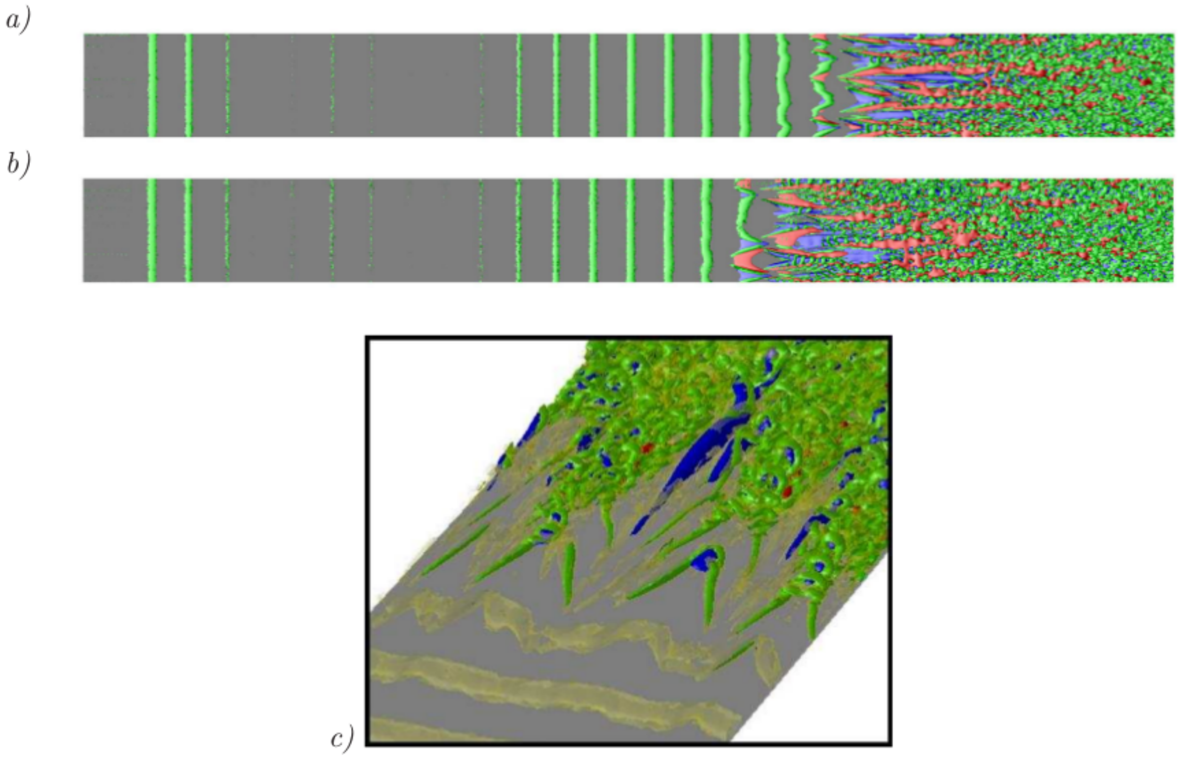

Fig. 2.11 : (color online) Flow visualizations in simulations of a ***Blasius boundary layer*** in the presence of forcing (Schlatter *et al.* 2010). (a) and (b) : top view, the flow is from left to right. Green isocontours show high vorticity regions. Red and blue isocontours show regions of positive and negative streamwise disturbance velocity $u_x = \pm 0.07 U_0$ with U_0 the far-field streamwise velocity. (c) : 3D view. The transparent yellow iscontours show 'high vorticity regions' of an intensity which corresponds to the green isocontours of (a) and (b), the green isocontours show regions of even higher vorticity. Red and blue isocontours show $u_x = \pm 0.1 U_0$. Observe a ***progressive transition to turbulence*** with **2D *TS waves*** then **3D Λ-*vortices***.

soon, in terms of x, into turbulence...

In cases of the first type described hereabove, where the level of turbulence in the inflow is low, and TS waves do play a role at the beginning, as in figure 2.11, the so-called ***'e^N method'*** has been proposed to estimate the location of the region where the flow becomes turbulent (see e.g. Mack 1977; Van Ingen 2008). In this method, one performs a ***local spatial stability analysis*** of the base flow, for a range of angular frequencies ω, to determine, as a function of the streamwise coordinate x, the spatial growth rates

$$- k_i(x,\omega) \tag{2.85}$$

of the corresponding TS waves. For a given ω, the wave starts to be amplified, i.e., $k_i(x,\omega)$ becomes negative, as soon as x exceeds a particular value $x_0(\omega)$. For $x > x_0(\omega)$, when x increases by dx, one expects that the amplitude A of the wave increases by dA with, according to (2.84),

$$\frac{A+dA}{A} \;=\; \exp(-k_i(x,\omega)\; dx) \quad\Longleftrightarrow\quad d\ln A \;=\; -\,k_i(x,\omega)\; dx\;. \tag{2.86}$$

Assuming that, at $x = x_0(\omega)$, the TS wave has an amplitude

$$A(x = x_0(\omega)) \;=\; A_0\;, \tag{2.87}$$

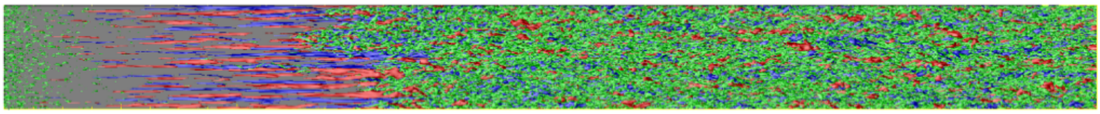

Fig. 2.12 : (color online) Flow visualization as figure 2.11 *a*, in a similar case where, however, a 'strong' 3D noise has been added in the inflow (Schlatter *et al.* 2010). Observe a ***bypass*** or ***'direct' transition to turbulence***, at a very short distance from the 'inlet', at least, much shorter than in the case of figure 2.11 *a*.

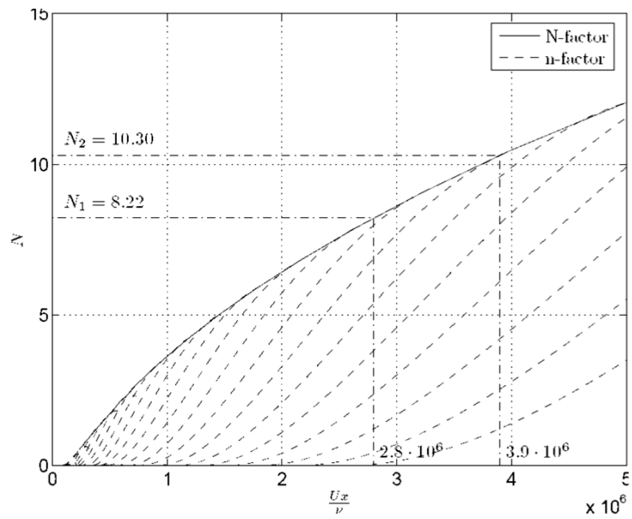

Fig. 2.13 : Illustration of the ***'e^N method'***, from Van Ingen (2008). For the Blasius boundary layer, the dashed curves show the amplification factors $n(x, \omega)$ of various TS waves, the continuous curve the maximum amplification factor $N(x)$.

we expect that at a distance x downstream, it has a larger amplitude

$$A(x) \; = \; A_0 \;\; e^{n(x,\omega)} \quad \text{with} \quad n(x,\omega) \; = \; \int_{x_0(\omega)}^{x} -k_i(x',\omega)\; dx' \tag{2.88}$$

the ***'amplification factor'*** of the wave. By calculating n as a function of x for a range of frequencies, one gets a set of n-curves; the envelope of these curves gives the ***maximum amplification factor***

$$N(x) \; = \; \max_{\omega} n(x,\omega) \tag{2.89}$$

which occurs at any x. This process is illustrated on the figure 2.13. The idea of the method is that transition to turbulence occurs when this maximum amplification factor, which is an increasing function of x, exceeds a limit

$$N(x) \; > \; N_{\rm lim} \quad \Longleftrightarrow \quad x \; > \; x_{\rm lim} \; . \tag{2.90}$$

If a 'good' correlations is used to estimate $N_{\rm lim}$, this method gives 'good' results for $x_{\rm lim}$ ... even for ***airfoils*** at high Reynolds number, as demonstrated recently by Sørensen & Zahle (2014) !.. To be more precise, Mack (1977) for instance proposed that the 'initial' value of the amplitude A_0 of the TS waves scales with the ***freestream turbulence level***

$$Tu \; = \; \frac{\sqrt{2k/3}}{U_0} \tag{2.91}$$

with k the average turbulent kinetic energy in the up and freestream, according to

$$A_0 \;\simeq\; A_0' \; Tu^a \; . \tag{2.92}$$

He proposed then that transition to turbulence occurs when

$$\begin{aligned} A(x) \gtrsim A_c \iff e^{N(x)} \gtrsim \frac{A_c}{A_0} &\iff N(x) \gtrsim \ln A_c - \ln A_0 \simeq \ln A_c - \ln A_0' - a \ln Tu \\ &\iff N(x) \gtrsim -8.43 - 2.4 \ln Tu \; , \end{aligned} \tag{2.93}$$

given the specific values chosen for all parameters on the basis of experimental results, that concerned the Blasius boundary layer.

2.6 Exercise and problem

Exercise 2.7 ***3D linear stability analysis of 2D viscous open shear flows: Squire's transformation and theorem***

Let us consider a ***2D viscous open shear flow*** defined as in the lectures by

$$\mathbf{v} \;=\; \mathbf{v}_0 \;=\; U(z)\,\mathbf{e}_x \; , \quad p \;=\; p_0 \;=\; -\,Gx \; , \tag{2.94}$$

where the modified pressure p contains gravity effects, and the flow domain is limited by 'plates' at $z = z_\pm$. The fluid is incompressible. The novelty of this exercise is that we consider small ***3D perturbations*** such that

$$\mathbf{v} \;=\; \mathbf{v}_0 \;+\; \mathbf{u} \; , \quad p \;=\; p_0 \;+ \widetilde{p} \tag{2.95}$$

where $\mathbf{u}$ and $\widetilde{p}$ depend on (x, y, z, t), and u_y may not vanish. Thus, we do not use a streamfunction, nor eliminate the pressure.

1 Write the linearized mass conservation and momentum equations (under vectorial form for this later) that govern the fate of $\mathbf{u}$ and $\widetilde{p}$, rendered dimensionless like in the lectures. Do not use special notations to signal dimensionless variables. Recall the definition of the control parameter R.

2 Is this initial-value problem isotropic in the xy plane ?

3 Let us consider a ***complex 3D normal mode of perturbation*** such that

$$\begin{aligned} \mathbf{u} \;&=\; [u(z)\,\mathbf{e}_x \;+\; v(z)\,\mathbf{e}_y \;+\; w(z)\,\mathbf{e}_z] \;\exp(ik_x x + ik_y y + \sigma t) \; , & (2.96a) \\ \widetilde{p} \;&=\; P(z) \;\exp(ik_x x + ik_y y + \sigma t) \; , & (2.96b) \end{aligned}$$

with k_x , k_y the wavenumbers of the mode in the x and y directions.
Establish the 4 linear ordinary differential equations that define the ***eigenproblem*** that determines the eigenfunctions $u,\ v,\ w$ and $P(z)$, up to a normalization factor, together with the temporal eigenvalue σ.
Explain why this is a ***generalized*** *eigenvalue problem.*

4 For a ***2D xz normal mode*** with $v = 0$ and $k_y = 0$, establish the 3 linear ordinary differential equations that define the ***eigenproblem*** that determines the eigenfunctions $u,\ w$ and $P(z)$, up to a normalization factor, together with the temporal eigenvalue σ.

5 Following Squire (1933), coming back to a ***3D normal mode*** (2.96) with $k_x > 0$ and $k_y \neq 0$, show that, with

$$\tilde{k}^2 \ = \ k_x^2 + k_y^2 \ , \quad \tilde{k}\tilde{u} \ = \ k_x u + k_y v \ , \quad \tilde{w} \ = \ w \ , \quad \tilde{P} \ = \ \tilde{k} P / k_x \ , \tag{2.97}$$

one can define (this is the so-called ***Squire's transformation*** !) a corresponding **2D *normal mode*** that has the temporal eigenvalue

$$\tilde{\sigma} \ = \ \sigma / \alpha \ , \tag{2.98}$$

at the Reynolds number

$$\tilde{R} \ = \ \alpha \ R \ , \tag{2.99}$$

with α a simple real function of k_x and $\tilde{k}$ that you will determine.

§

We admit that ***2D yz normal modes*** with $k_x = 0$ are always damped.

§

6 Show the ***Squire's theorem***: if there exists a critical Reynolds number R_c above which this viscous OSF is linearly unstable, the wave that first become amplified at $R > R_c$ is necessarily ***2D xz***.

Problem 2.2 ***Spatial linear stability analysis - The case of plane Poiseuille flow***

We consider a ***viscous parallel open shear flow*** with a velocity field

$$\mathbf{v} \ = \ \mathbf{v}_0 \ = \ U(z) \ \mathbf{e}_x$$

and investigate its ***stability*** versus ***2D xz perturbations***. With the use of the dimensionless units described in the Lecture Notes, the wall-normal coordinate z varies in the interval $[-1, +1]$. Our aim is to perform a ***spatial stability analysis***, i.e. to compute modes of the form (2.100) with $\omega \in \mathbb{R}^*$, $k \in \mathbb{C}^*$.

1 Give the linearized ordinary differential equation (ODE) that determines the modes of this problem, written under the form

$$\mathbf{u} \ = \ \mathbf{v} \ - \ \mathbf{v}_0 \ = \ \mathbf{curl}(\psi \ \mathbf{e}_y) \quad \text{with} \quad \psi \ = \ \Psi(z) \ \exp[i(kx - \omega t)] \ . \tag{2.100}$$

Recall the physical origin of this equation, that you will write as an equation applied to $\Psi(z)$. You should introduce the operator

$$D \ = \ \partial_z$$

and the notation $r = R^{-1}$ with R the Reynolds number. You should normalize your equation such that only positive powers of k appear. What is the highest power of k that intervenes ?

2 In order to decrease this power, implement the change of unknown function

$$\Psi(z) \ = \ \Phi(z) \ e^{-kz} \quad \Longleftrightarrow \quad \Phi(z) \ = \ \Psi(z) \ e^{kz} \ .$$

First, calculate $D\Psi$, $D^2\Psi$, $(D^2-k^2)\Psi$ and $(D^2-k^2)^2\Psi$ in terms of Φ and its derivatives[5]. Second, show that $\Phi(z)$ verifies an ODE where k appears only up to the second power.

3 In order to obtain an ***eigenvalue problem*** on k, we introduce the vector

$$v \;=\; \begin{bmatrix} v_1 \\ v_2 \end{bmatrix} \;=\; \begin{bmatrix} k\Phi(z) \\ \Phi(z) \end{bmatrix} \; . \tag{2.101}$$

Show that the ODE on $\Phi(z)$ established Q.2 can be written under the form

$$L_1 \cdot v_1 \;+\; L_2 \cdot v_2 \;=\; kD_1 \cdot v_1 \tag{2.102}$$

where you will identify the differential operators L_1 of order 3, L_2 of order 4, D_1 of order 2, which may depend on ω, r and U but not on k.

Indication: you should show that one may assume $L_2 = -rD^4 - i\omega D^2$.

4 Check that the relation of proportionality of the two components of v and the ODE on $\Phi(z)$ can be written under the matrix form

$$\begin{bmatrix} L_1 & L_2 \\ 1 & 0 \end{bmatrix} \cdot v \;=\; k \begin{bmatrix} D_1 & 0 \\ 0 & 1 \end{bmatrix} \cdot v \; . \tag{2.103}$$

From now on, the basic flow is the ***plane Poiseuille flow*** $U(z) = 1 - z^2$. Also, there are walls at $z = \pm 1$.

5 Recall the boundary conditions that ψ and Ψ must satisfy. Establish the boundary conditions that Φ must satisfy.

6 In order to solve with a ***spectral method*** the system (2.103), justify that it is reasonable to search $\Phi(z)$ as an expansion of the form

$$\Phi(z) \;=\; \sum_{n=1}^{N_z} \Phi_n F_n(z) \quad \text{with} \quad F_n(z) \;=\; (z^2-1)^2 \; T_{n-1}(z) \; , \tag{2.104}$$

T_n the n^{th} Chebyshev polynomial of the first kind.

7.1 With the notations of equation (2.101), we assume

$$v_1 \;=\; \sum_{n=1}^{N_z} a_n F_n(z) \; , \quad v_2 \;=\; \sum_{n=1}^{N_z} \Phi_n F_n(z) \; ,$$

and introduce the vector of the spectral coefficients

$$V \;=\; \begin{bmatrix} V_1 \\ V_2 \end{bmatrix} \;=\; \begin{bmatrix} a_1 \\ \vdots \\ a_{N_z} \\ \Phi_1 \\ \vdots \\ \Phi_{N_z} \end{bmatrix} \;\in\; \mathbb{C}^{2N_z} \; .$$

[5] In order to simplify, we denote $D\Psi$ what we could also denote $D \cdot \Psi$.

We also introduce, to discretize the equation (2.102), the collocation points

$$z_m \;=\; \cos[m\pi/(N_z+1)] \quad \text{for} \quad m \in \; \{1,2,\cdots,N_z\}\ .$$

For $N_z = 9$, with the help of a geometrical construction that uses the unit circle, represent these points in the interval $[-1,1]$, and comment.

7.2 Show that the system (2.103) can be represented by the matrix system

$$ML \cdot V \;=\; k\ MD \cdot V \tag{2.105}$$

with

$$ML \;=\; \begin{bmatrix} ML1 & ML2 \\ Id & 0 \end{bmatrix}\ , \quad MD \;=\; \begin{bmatrix} MD1 & 0 \\ 0 & Id \end{bmatrix}\ ,$$

Id being the identity matrix of dimension $N_z \times N_z$, $ML1$, $ML2$ and $MD1$ being square matrices that represent the operators L_1, L_2 and D_1 defined in Q.3. You will establish the expressions of the matrix elements at line m and column n of $ML1$, $ML2$ and $MD1$.

8 Using a Mathematica code of a structure similar to the one of problem 2.1, construct the matrices ML and MD for a given value of N_z, `Nz` in your code[6]. Hereafter is its skeleton:

```
(*Number of base functions*) Nz= 36;
(*Base functions*) F[n_,z_]= ...
(*Collocation points*) z[m_]= Cos[m Pi/(Nz+1.)]
(*Inverse of the Reynolds number*) r= 1/R;
(*Base flow*) U[z_]= 1-z^2;
(*Operators*) Dz[f_]:= D[f,z]; Dz2[f_]:= ... ; Dz3[f_]:= ... ; Dz4[f_]:= ... ;
L1[f_]:= 4 r Dz3[f] + ...
L2[f_]:= -r Dz4[f] - ...
D1[f_]:= ...
(*Kronecker delta*) delta[i_,j_]:= If[i==j, 1, 0]

(*Matrices*) MatD = MatL = IdentityMatrix[2 Nz];
Do[
   Do[
      MatD[[m,n]] = ReplaceAll[ ... , z->z[m]];
      MatL[[m,n]] = ReplaceAll[ ... , z->z[m]];
      MatL[[m,Nz+n]] = ReplaceAll[ ... , z->z[m]];
      MatL[[Nz+m,n]] = ... ;
      MatL[[Nz+m,Nz+n]] = ...
     ,{m,1,Nz}]
  ,{n,1,Nz}]
MD[R_]= MatD; ML[omega_,R_]= MatL;

kspectrum[omega_,R_]:= Eigenvalues[{ML[omega,R], MD[R]}]
```

Check that, when $\omega = \omega_{ct} = 0.269$, $R = R_{ct} = 5772$ computed with the temporal stability analysis, you recover in the k-spectrum a wavenumber k close to $k_{ct} = 1.02$, the critical wavenumber found with the temporal stability analysis. For this purpose, use the command

[6] You may test your code at the beginning with 'small' values of N_z, but the preferred value that you must use is $N_z = 36$.

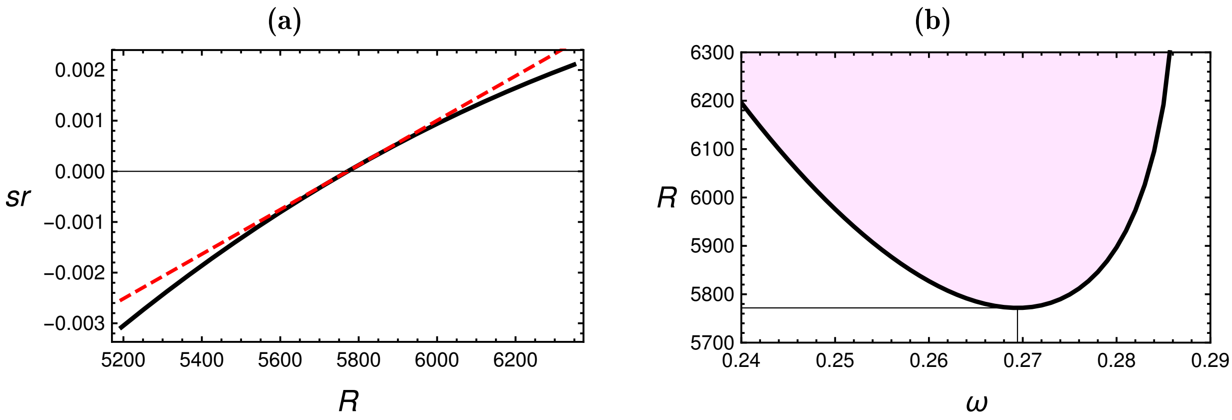

Fig. 2.14 : DIY ! According to the ***spatial stability analysis*** performed in the problem 2.2, **a:** the continuous curve shows the ***spatial growth rate*** of the most relevant spatial mode with the critical angular frequency, the dashed line the lowest order estimate ϵ/ℓ_0 ; **b:** region of ***linear instability of PPF to TS waves***; the straight lines show the critical parameters.

```
kclose[omega_,R_]:= Select[ kspectrum[omega,R], Abs[# - kct] < 0.2 &][[1]]
```

9 Check that, when R varies from $0.9R_{ct}$ to $1.1R_{ct}$, this mode becomes amplified in space. For this purpose calculate theoretically, compute and then plot figure 2.14a the ***spatial growth rate*** sr of this mode (define a function `sr[omega,R]` that depends on `kclose[omega,R]`) vs R.

10 Code with `FindRoot` the computation of the ***neutral Reynolds number*** $R_1(\omega)$ at which $sr(\omega, R)$ vanishes. Construct a list `lomR1` of the couples $(\omega, R_1(\omega))$ for discrete ω values spanning the interval

$$0.24 \ \leq \ \omega \ \leq \ 0.286 \ ,$$

and plot figure 2.14b the corresponding ***spatial neutral curve***.

11 Code with `FindMinimum` the computation of the ***bifurcation point*** where the first spatially amplified mode appears, for the lowest value of R. Compare the ***critical parameters*** (ω_c, k_c, R_c) obtained with the ones determined with the temporal stability analysis. Comment.

12 Compute with 3 digits the ***characteristic length*** ℓ_0 such that close to onset, for $\epsilon = R/R_c - 1$ small,

$$sr(\omega_c, R_c) \ = \ \epsilon/\ell_0 \ + \ o(\epsilon) \ . \tag{2.106}$$

Check the relevance of this computation by overlaying a straight line onto figure 2.14a. Comment.

Bibliography

Abkar, M. & Porté-Agel, F. 2015 Influence of atmospheric stability on wind-turbine wakes: a large-eddy simulation study. *Phys. Fluids* **27**, 035104,1–19.

Ahlers, G., Grossmann, S. & Lohse, D. 2009 Heat transfer and large scale dynamics in turbulent Rayleigh-Bénard convection. *Rev. Mod. Phys.* **81**, 503–537, DOI: 10.1103/RevModPhys.81.503 - Lorraine Clic

Bergé, P., Pomeau, Y. & Vidal, C. 1984 *Order within Chaos: Towards a Deterministic Approach to Turbulence*. John Wiley & Sons.

Bodenschatz, E., Pesch, W. & Ahlers, G. 2000 Recent developments in Rayleigh-Bénard Convection. *Annu. Rev. Fluid Mech.* **32**, 709–778.

Busse, F. H. 2003 The sequence-of-bifurcations approach towards understanding turbulent fluid flow. *Surveys in Geophys.* **24**, 269–288.

Davis, G. D. V. 1983 Natural convection of air in a square cavity: a benchmark numerical solution. *Int. J. Numer. Methods Fluids* **3**, 249–264, DOI: 10.1002/fld.1650030305 - Lorraine Clic

Drazin, P. D. 2002 *Introduction to hydrodynamic stability*. Cambridge University Press.

Haken, H. 1983 *Synergetics - An introduction*. Springer-Verlag.

Hu, Y., Ecke, R. & Ahlers, G. 1993 Convection near threshold for Prandtl numbers near 1. *Phys. Rev. E* **48**, 4399–4413, DOI: 10.1103/PhysRevE.48.4399 - Lorraine Clic

Huerre, P. & Rossi, M. 1998 Hydrodynamic instabilities in open flows. *Hydrodynamics and Nonlinear Instabilities* (ed. C. Godrèche & P. Manneville), pp. 81–294. Cambridge University Press.

Lorenz, E. 1963 Deterministic Nonperiodic Flow. *J. Atmospheric Sci.* **20**, 130–141, DOI: 10.1175/1520-0469(1963)020<0130:DNF>2.0.CO;2 - Open access

Mack, L. M. 1977 Transition and laminar instability. *NASA-CP* **153203**.

Plapp, B. B. 1997 Spiral pattern formation in Rayleigh-Benard convection. PhD thesis, Cornell University.

Plaut, E. 2008 *Modélisation d'instabilités : méthodes non linéaires*. Cours du Master 2 recherche de mécanique-énergétique de Nancy, http://emmanuelplaut.perso.univ-lorraine.fr/publisp

Plaut, E. 2020 *Mécanique des fluides 2 : ondes, couches limites et turbulence*. Cours de Mines Nancy (2A), http://emmanuelplaut.perso.univ-lorraine.fr/publisp

Plaut, E. & Busse, F. H. 2002 Low-Prandtl-number convection in a rotating cylindrical annulus. *J. Fluid Mech.* **464**, 345–363.

Plaut, E., Lebranchu, Y., Simitev, R. & Busse, F. H. 2008 Reynolds stresses and mean fields generated by pure waves: applications to shear flows and convection in a rotating shell. *J. Fluid Mech.* **602**, 303–326.

Plaut, E., Peinke, J. & Hölling, M. 2021 *Turbulence & Wind Energy*. Cours de Mines Nancy (3A), http://emmanuelplaut.perso.univ-lorraine.fr/publisp

Podvin, B. & Sergent, A. 2015 A large-scale investigation of wind reversal in a square Rayleigh-Bénard cell. *J. Fluid Mech.* **766**, 172–201, DOI: 10.1017/jfm.2015.15

Reynolds, O. 1895 On the dynamical theory of incompressible viscous fluids and the determination of the criterion. *Phil. Trans. Roy. Soc. Lond.* **186**, 123–164.

Schlatter, P., Deusebio, E., de Lange, R. & Brandt, L. 2010 Numerical study of the stabilisation of boundary-layer disturbances by finite amplitude streaks. *Int. J. Flow Control* **2**, 259–288, DOI: 10.1260/1756-8250.2.4.259

Schlüter, A., Lortz, D. & Busse, F. H. 1965 On the stability of steady finite amplitude convection. *J. Fluid Mech.* **23**, 129–144.

Schmid, P. J. & Henningson, D. S. 2001 *Stability and transition in shear flows*. Springer-Verlag.

Sørensen, N. N. & Zahle, F. 2014 Airfoil prediction at high Reynolds numbers using CFD. *10th European Fluid Mechanics Conference (EUROMECH)*. http://orbit.dtu.dk/ws/files/123876178/Airfoil_prediction_at_high_Reynolds_numbers_using_CFD.pdf

Squire, H. B. 1933 On the stability for threee-dimensional disturbances of viscous fluid flow between parallel walls. *Proc. R. Soc. London A* **142**, 621–628.

Stasiek, J. 1997 Thermochromic liquid crystals and true colour image processing in heat transfer and fluid-flow research. *Heat and Mass Transfer* **33**, 27–39, DOI: 10.1007/s002310050158 - Lorraine Clic

Van Ingen, J. L. 2008 *The e^N method for transition prediction: historical review of work at TU Delft*. AIAA, https://repository.tudelft.nl/islandora/object/uuid:e2b9ea1f-5fa1-47c0-82ad-64d1c74a5378